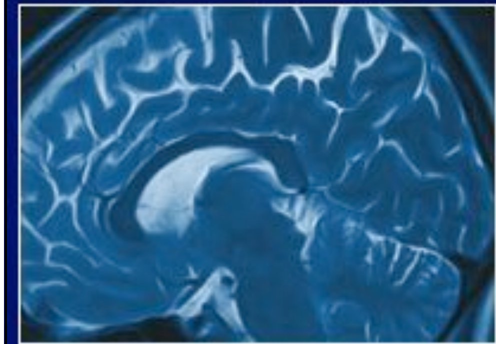

The Waisman Laboratory
for Brain Imaging and Behavior

Introduction to Computational Neuroanatomy

October 11, 2007

Moo K. Chung

Department of Biostatistics and Medical Informatics
Waisman Laboratory for Brain Imaging and Behavior
University of Wisconsin-Madison

http://www.stat.wisc.edu/~mchung

Acknowledgements

Shubing Wang, Kim Dalton, Daniel Kelley,
Richard Davidson

University of Wisconsin-Madison

Abstract

Needs for 2D cortical surface specific analysis framework in computational neuroanatomy are explained. The widely used Gaussian kernel smoothing in 3D whole brain volume morphometry assigns isotropic weights according to Euclidian distance but cortical surface data fail to be isotropic along the surface. On the curved surface, a straight line between two points is not the shortest distance so one may incorrectly assigns less weights to closer observations. To address this problem, 2D surface based smoothing is developed. The 3D whole brain volume based image normalization tend to misalign sulcal patterns across subjects. To avoid this problem, 2D surface based normalization is necessary.

Outline

Introduction

Image segmentation

Image normalization

Image smoothing

Statistical Model

Random field theory

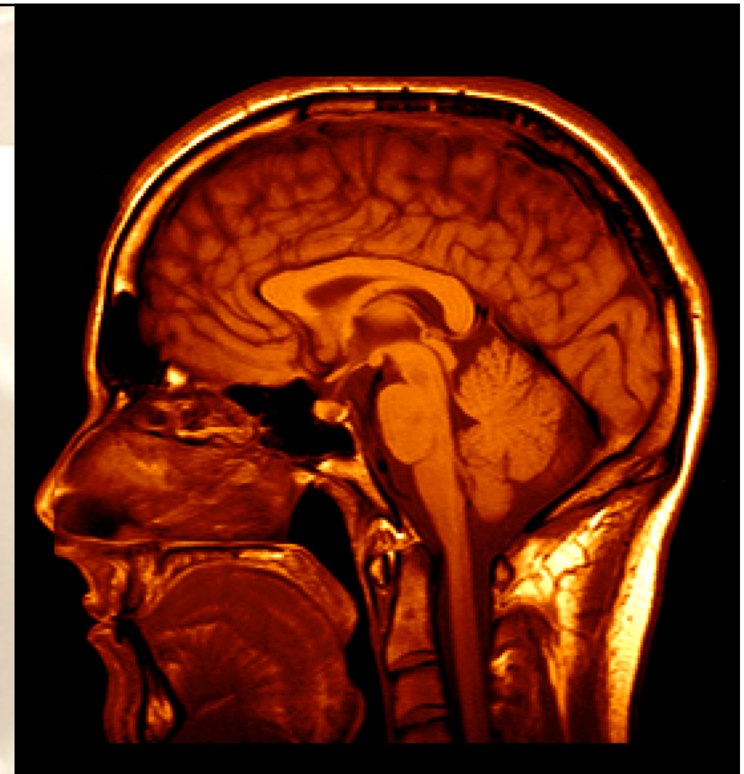

Data: 3D MRI

16 autistic subjects (15.93±4.71)

12 normal controls (17.08±2.78)

Right-handed males of similar ages.

Aim

Quantify structural abnormality in the autistic subjects.

Cortical anatomy

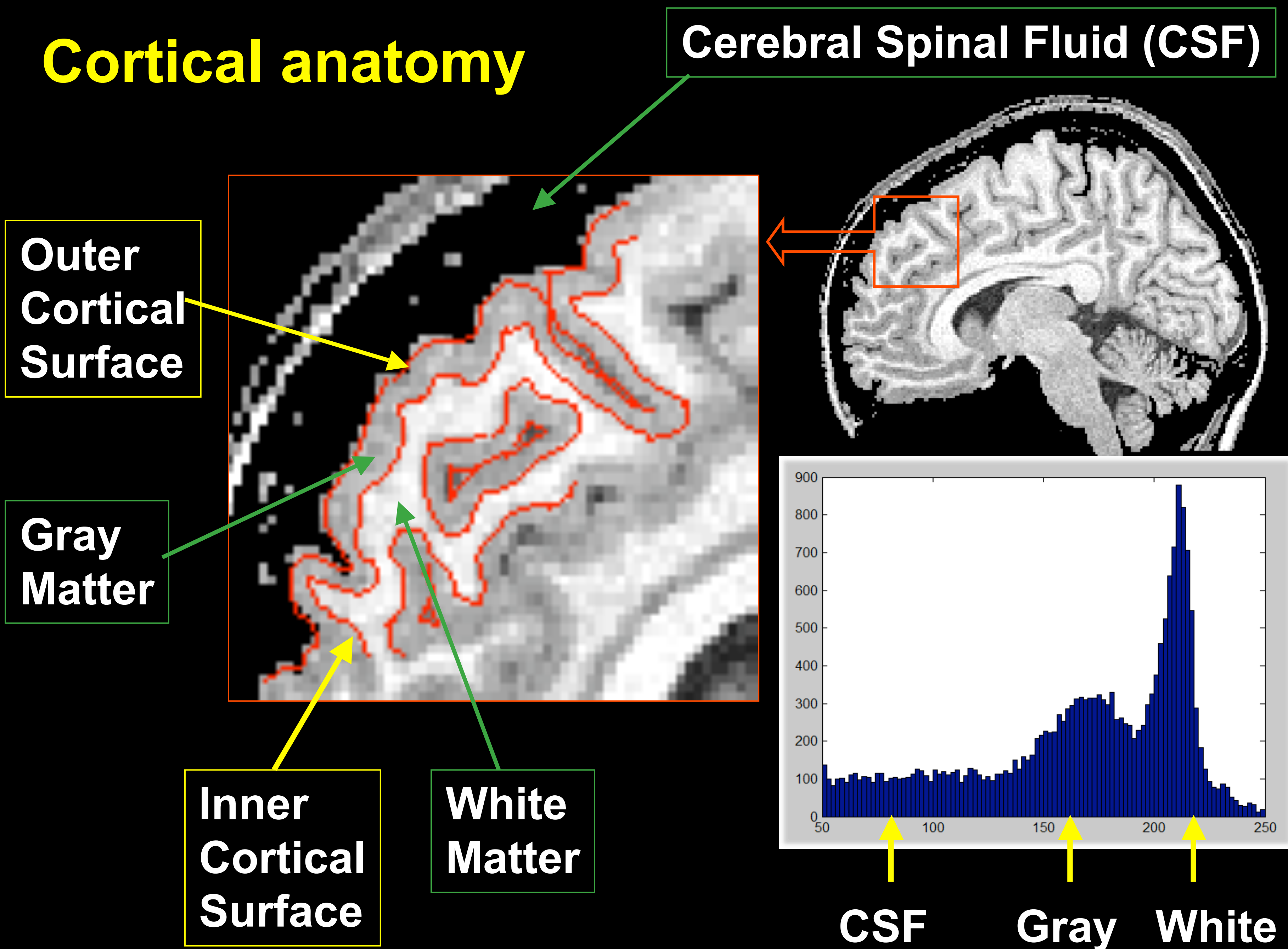

Image segmentation

Image intensity non-uniformity correction via MNI's N3 algorithm

Original MRI

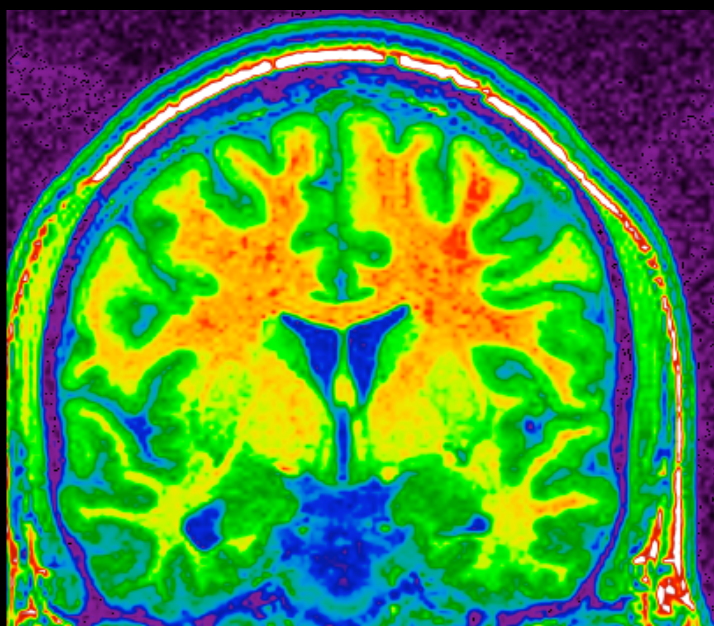

Corrected

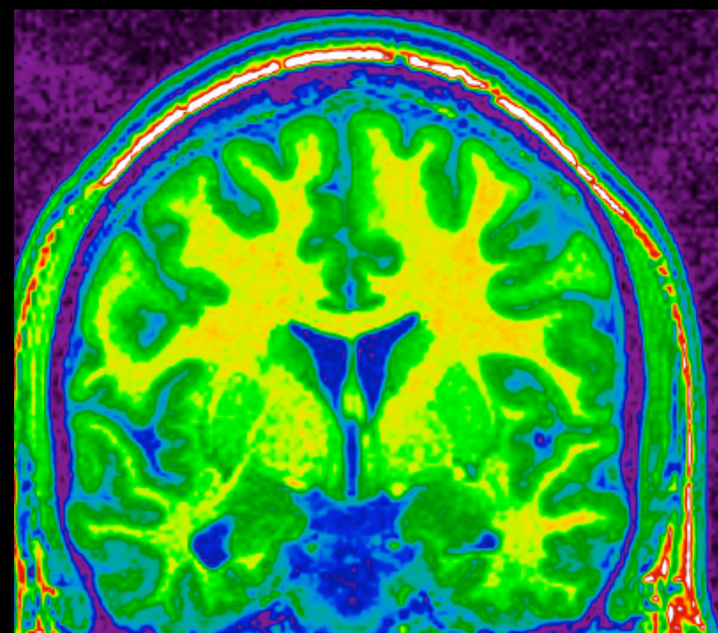

Gaussian mixture modeling

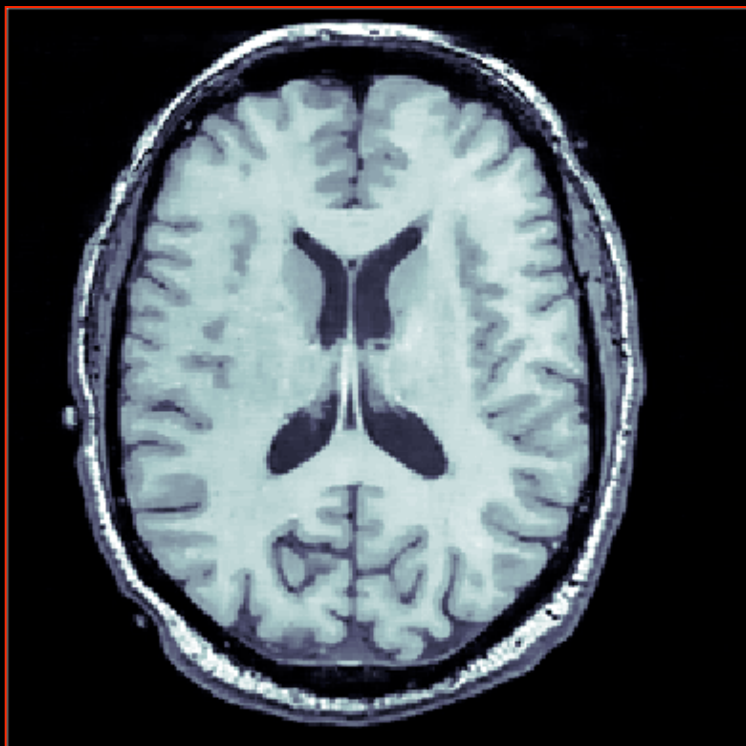

Skull stripping

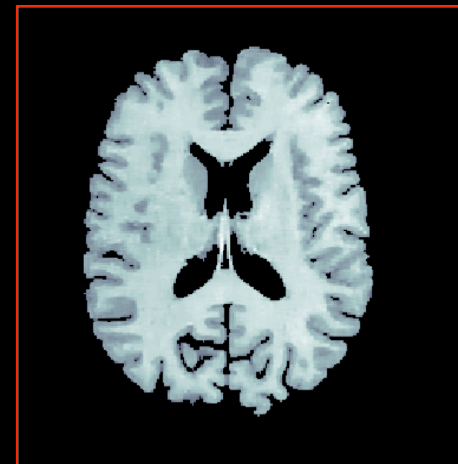

Segmentation

SPM approach

Gaussian mixture model

•Histogram-based parametric method.

•It directly model the image intensity histogram as a linear combination of independent Gaussian random variables.

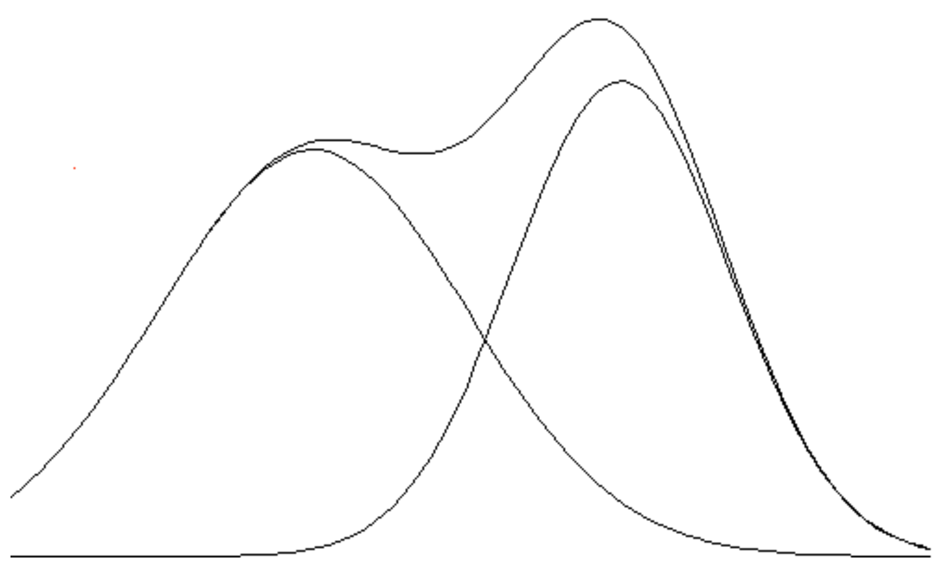

Histogram of sum of two Gaussian mixtures

MNI neural network classifier

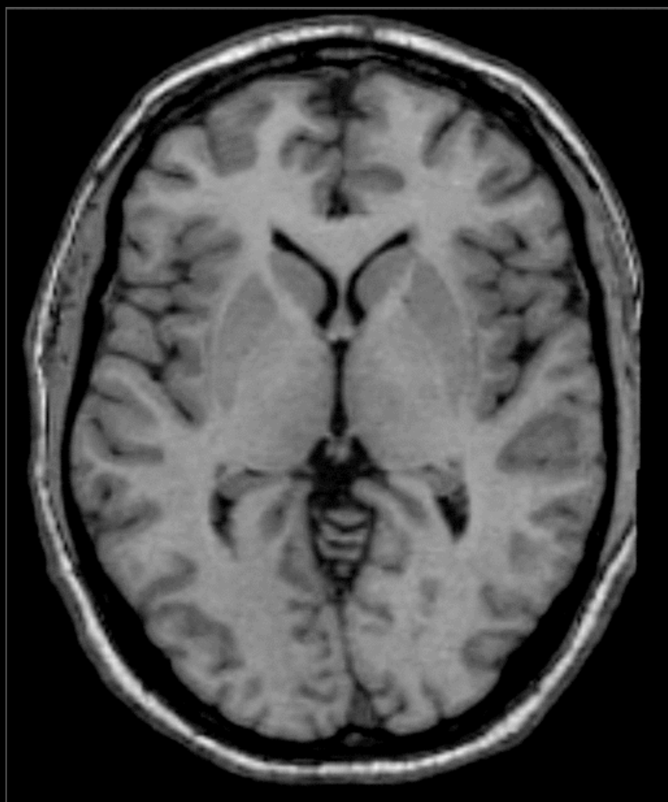

Original data

3 disjoint classes

Real brain

Computer generated

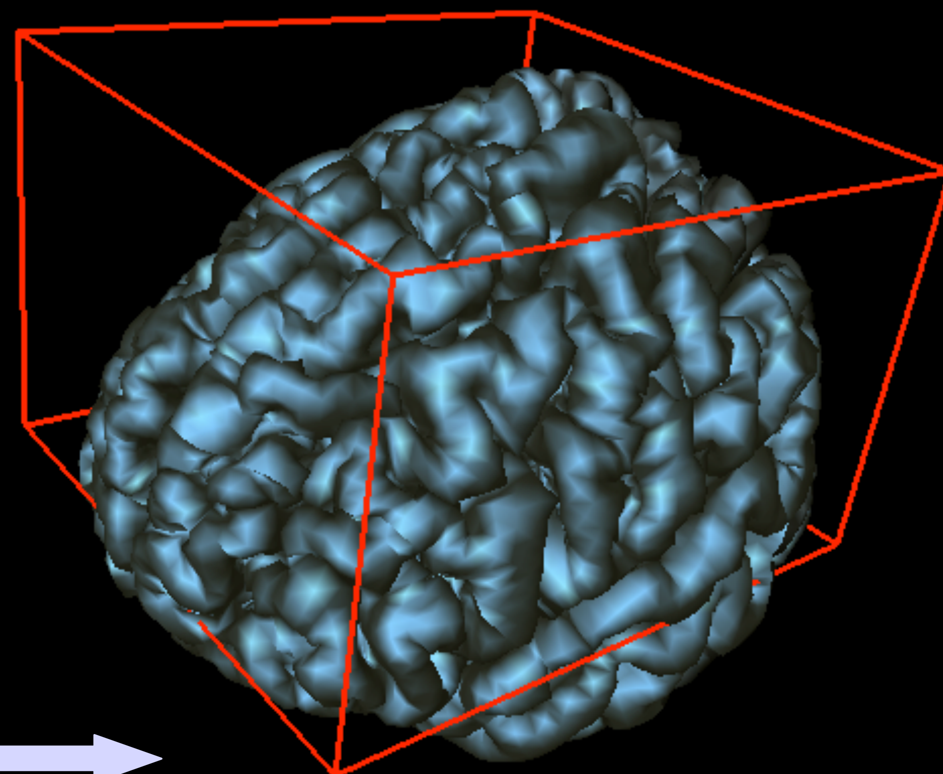

Cortical surface segmentation

Deformable surface algorithm (McDonalds *et al*., 2001. NeuroImage)

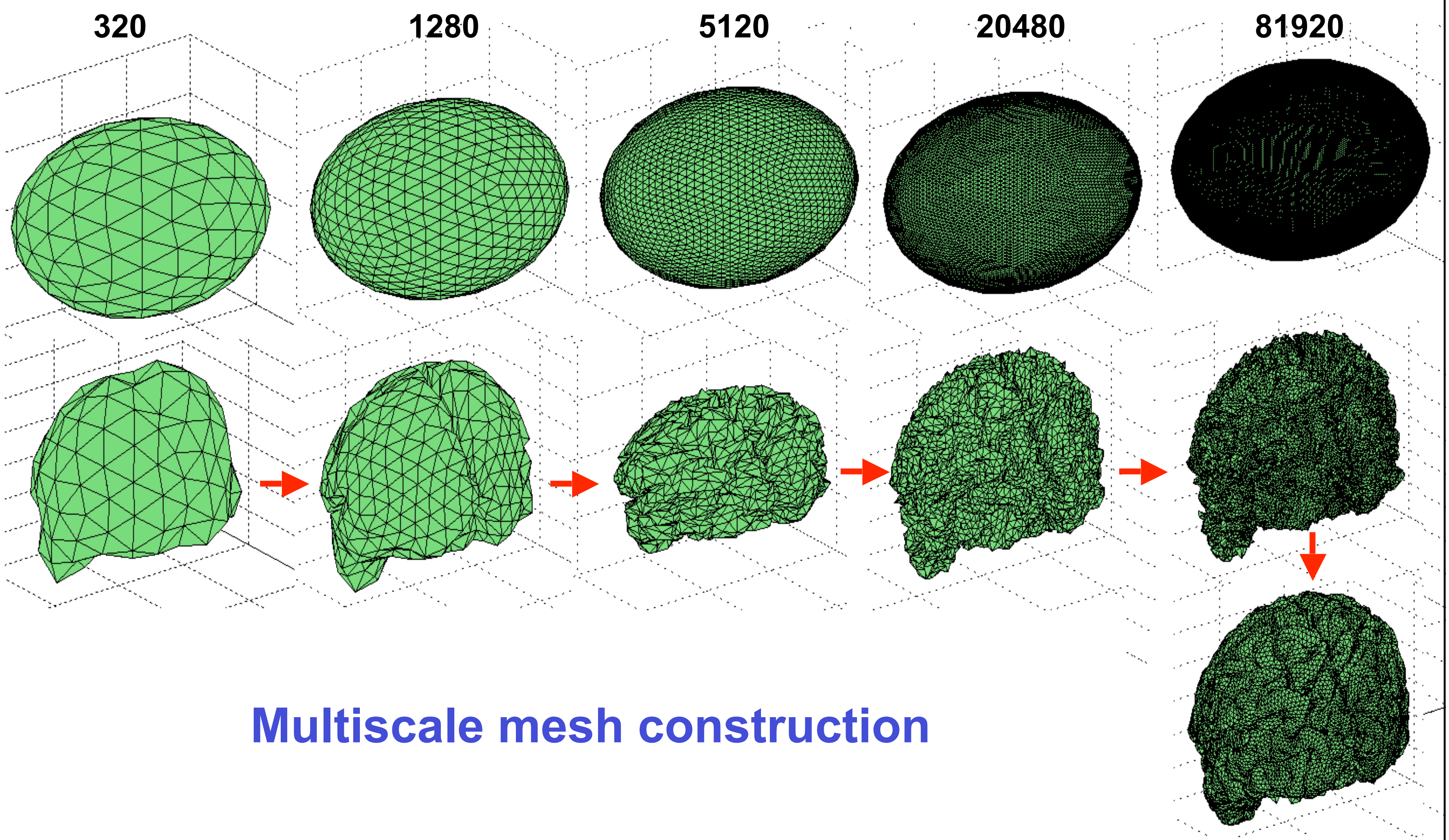

Multiscale mesh construction

Extracted cortical surfaces

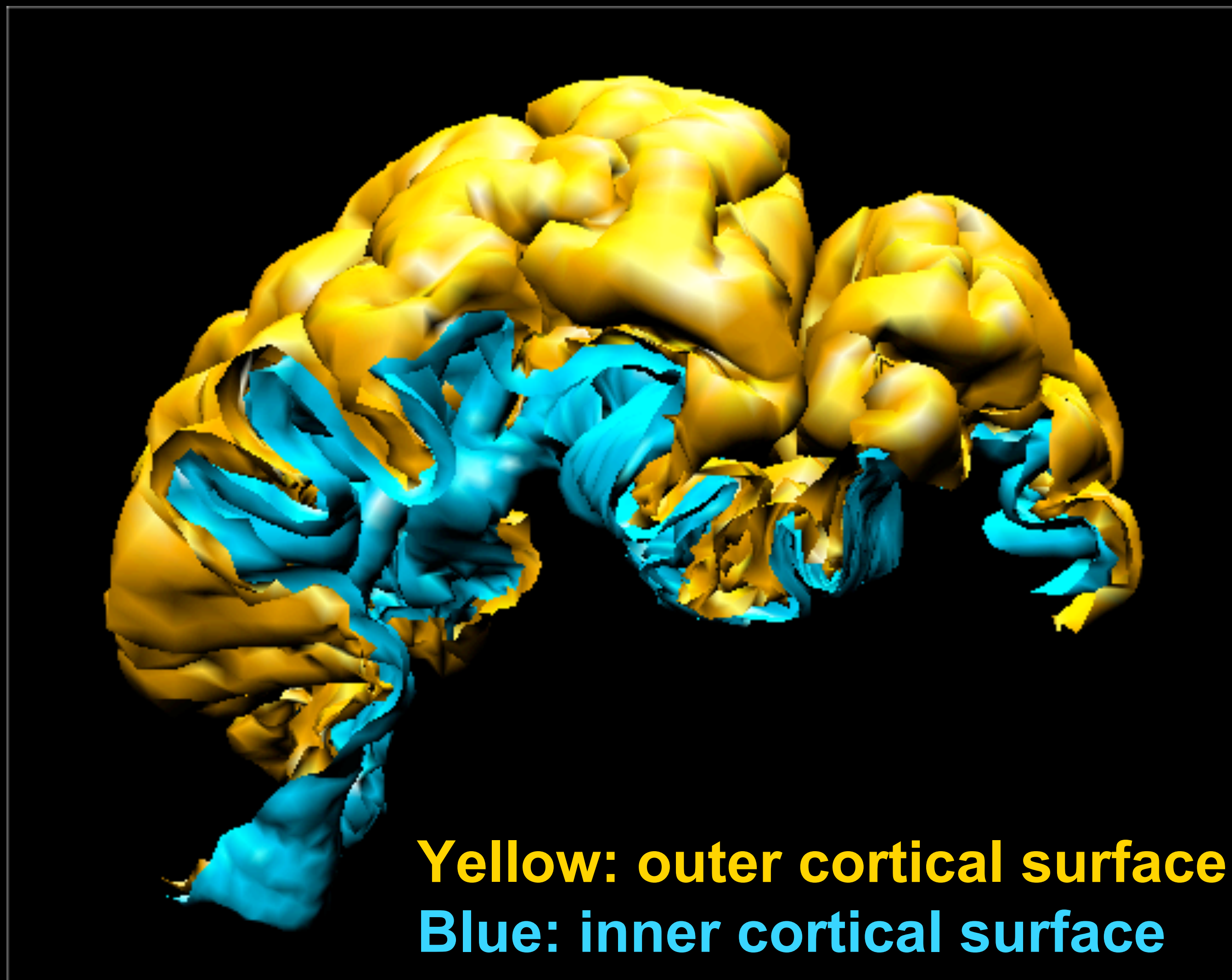

Cortical thickness = distance between surfaces

Polygonal mesh data

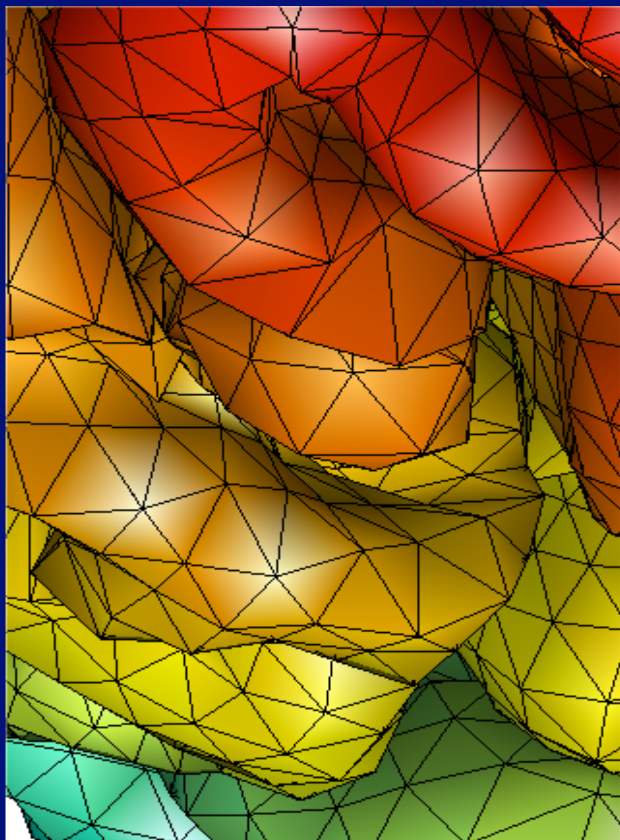

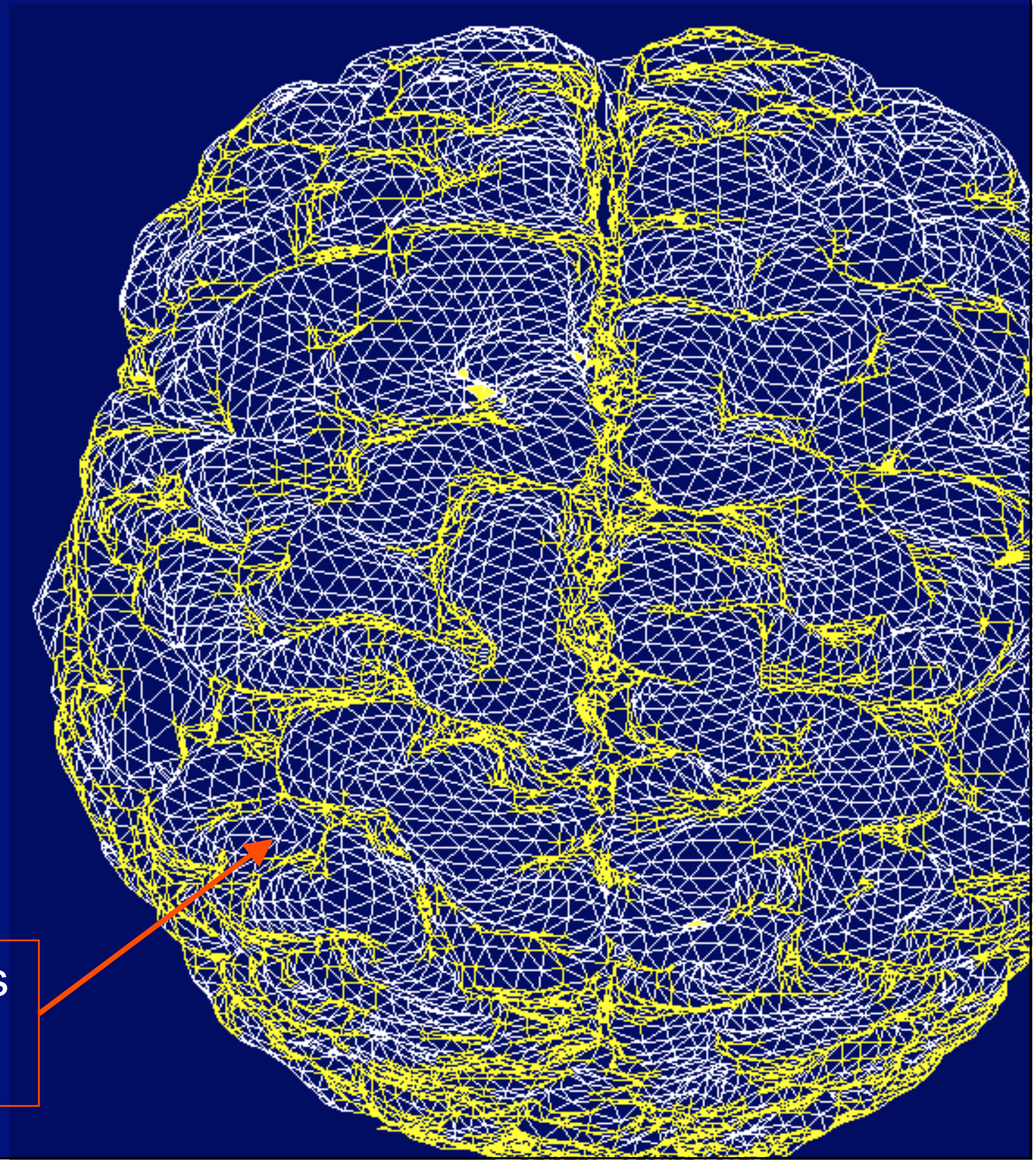

82,190 triangles

40,962 vertices

Ambiguity of measuring cortical thickness

thickness of gray matter is used as an anatomical index.

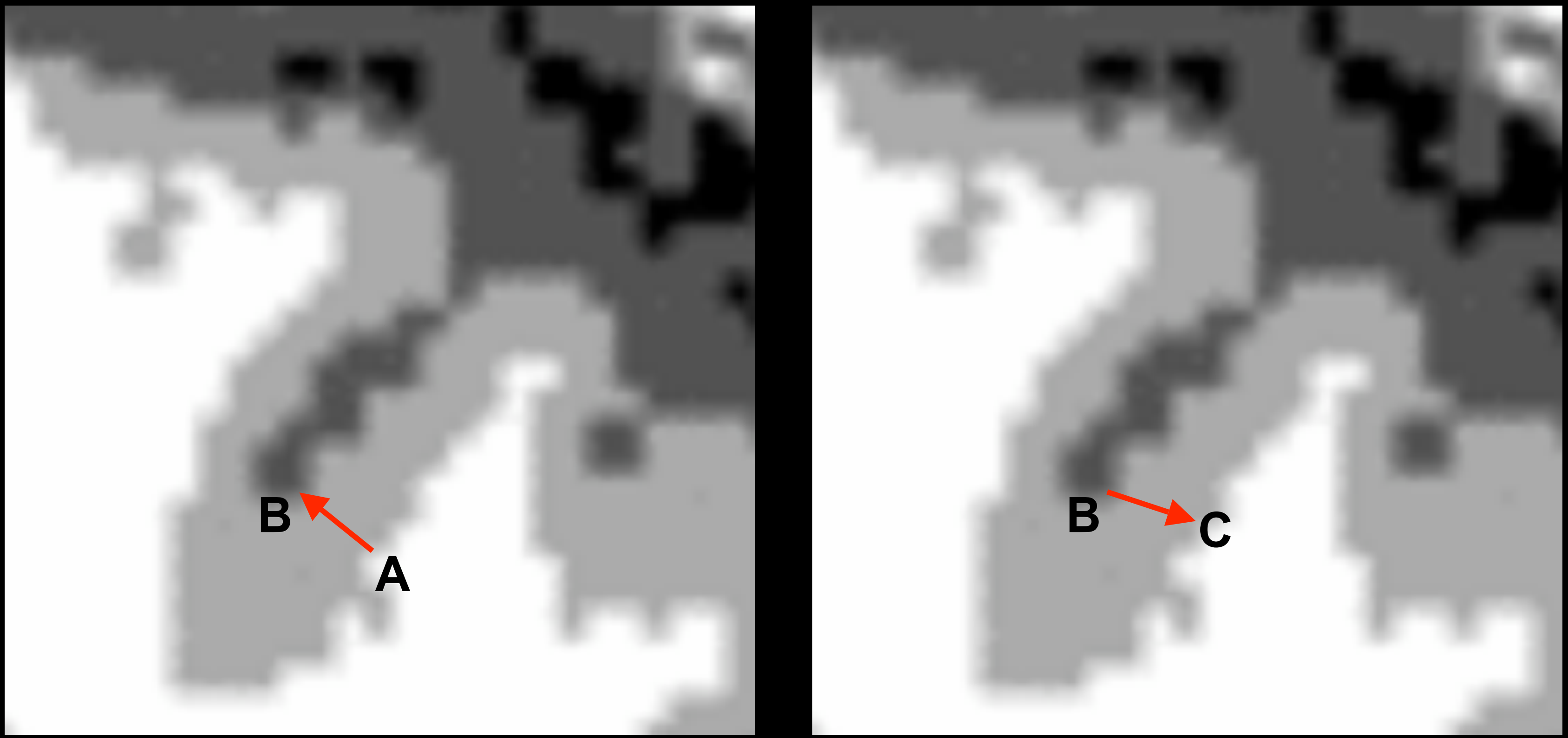

orthogonal projection from A to B

orthogonal projection from B to C

No less than 4 proposed methods of measuring thickness in literature

Cortical Thickness

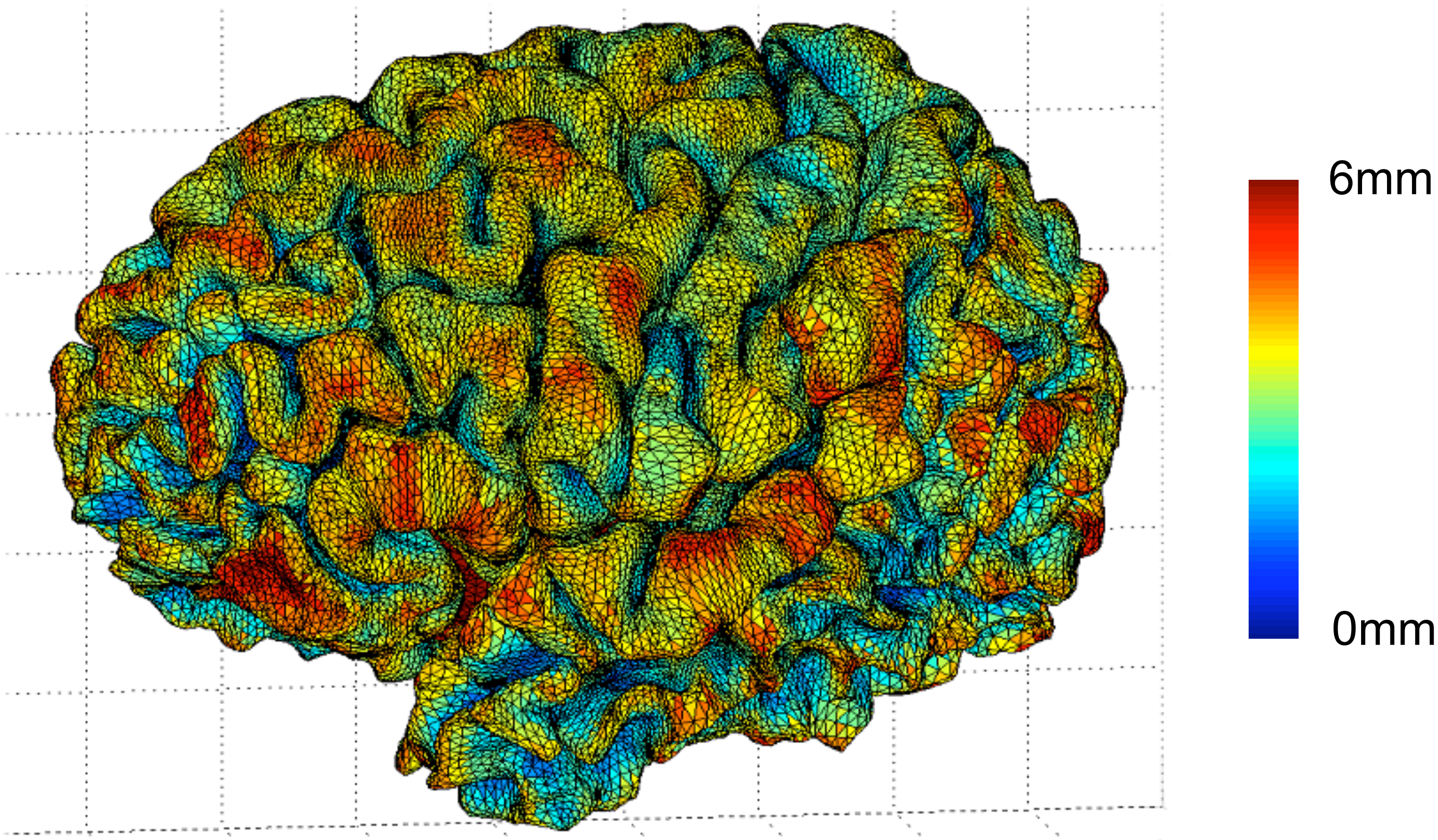

$$Y(p) = \theta(p) + \epsilon(p), p \in \partial\Omega$$

Cortical thickness is modeled as a Gaussian random field.

Cortical Thickness Dilatation (single subject, age = 14)

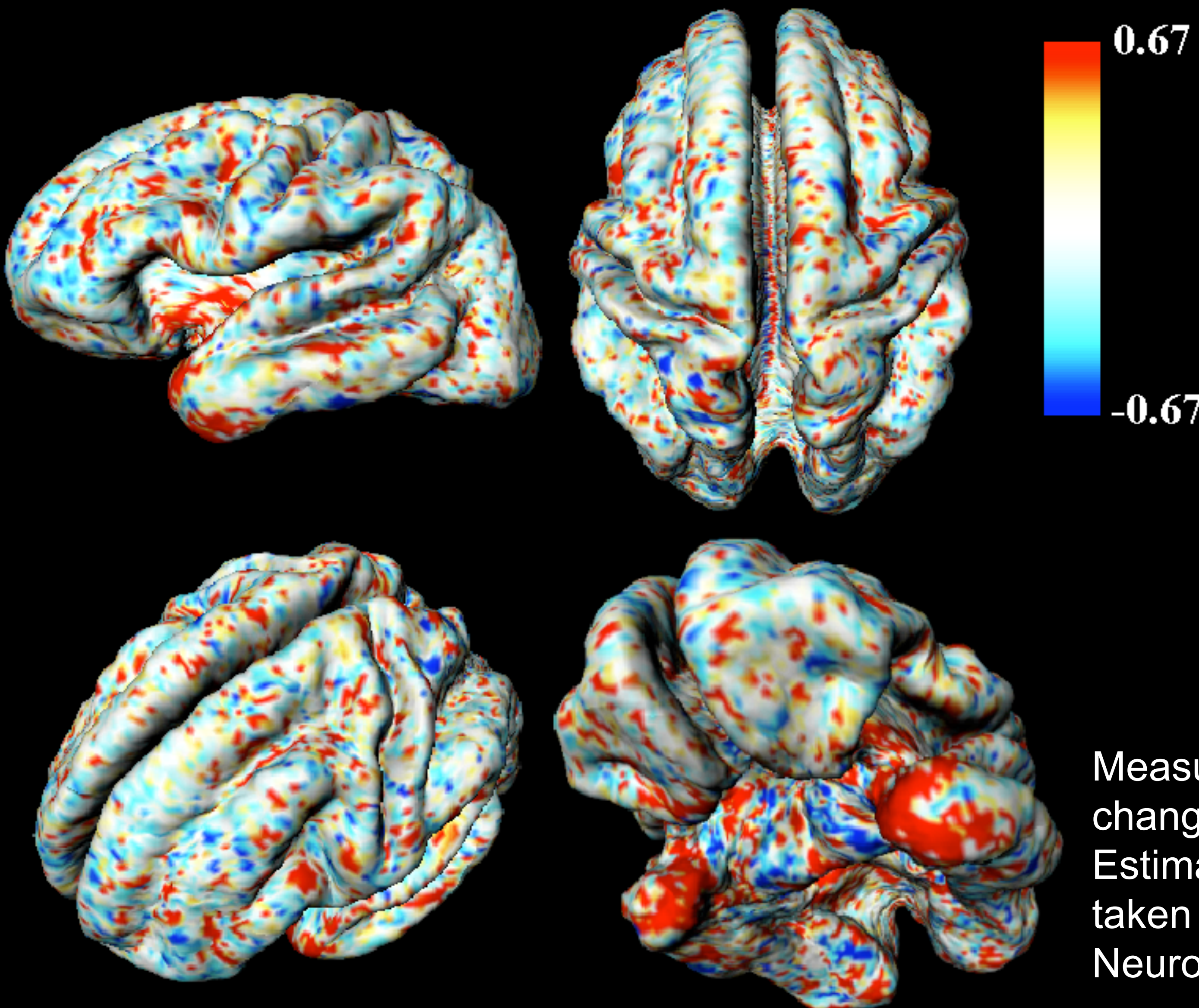

Measuring the rate of change over time.
Estimated using two scans taken at different time.
NeuroImage (2005)

Surface Normalization

Why not 3D whole brain volume registration ?

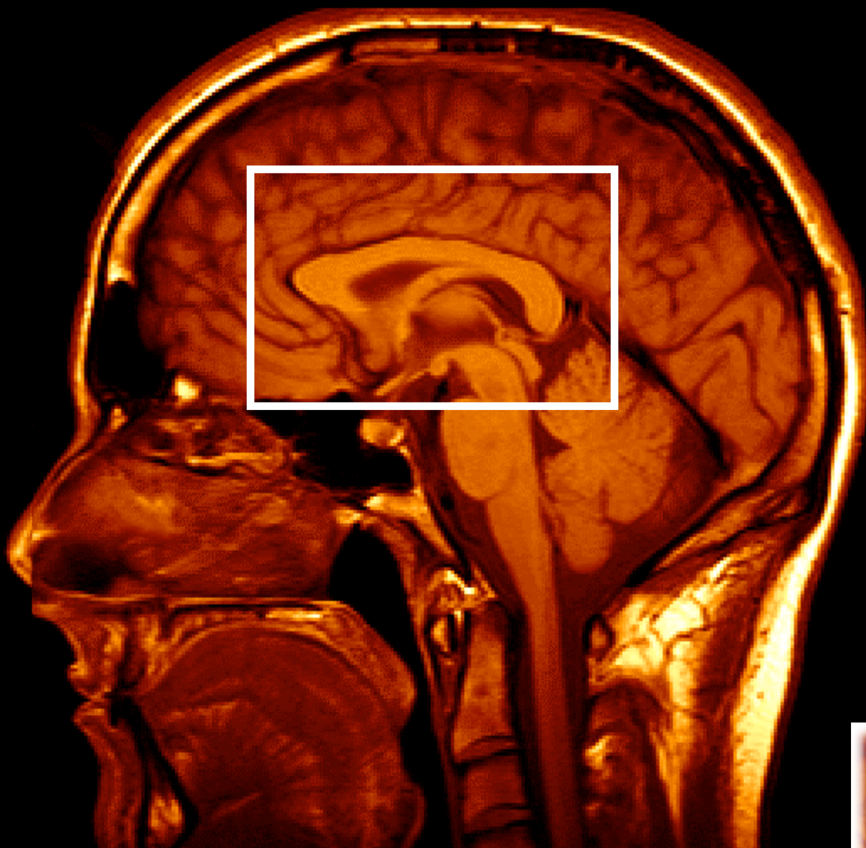

Each subject has different brain shape. So how do we compare across subjects?

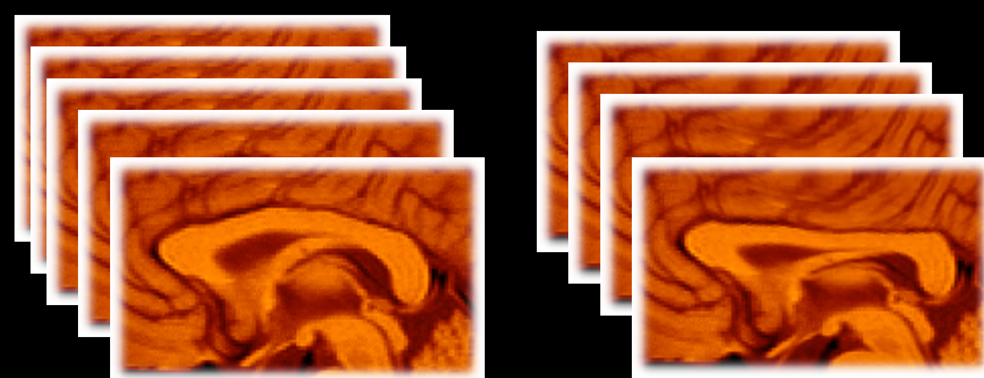

Group 1

Group 2

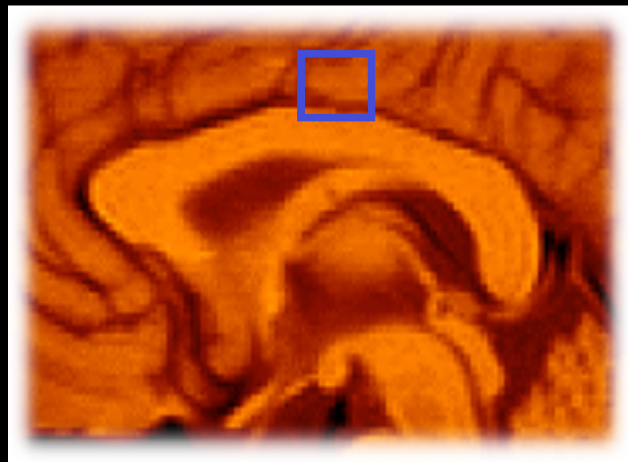 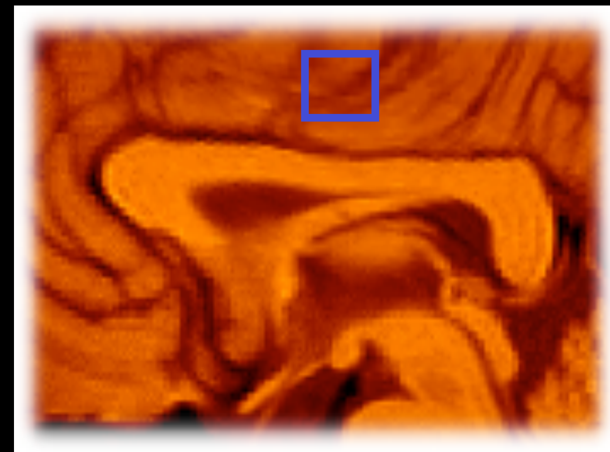

Voxel(pixel) by voxel(pixel) comparison causes anatomical mismatching.

Image registration. The aim of image registration is to find a smooth one-to-one mapping that matches homologous anatomies together.

Deformable template framework

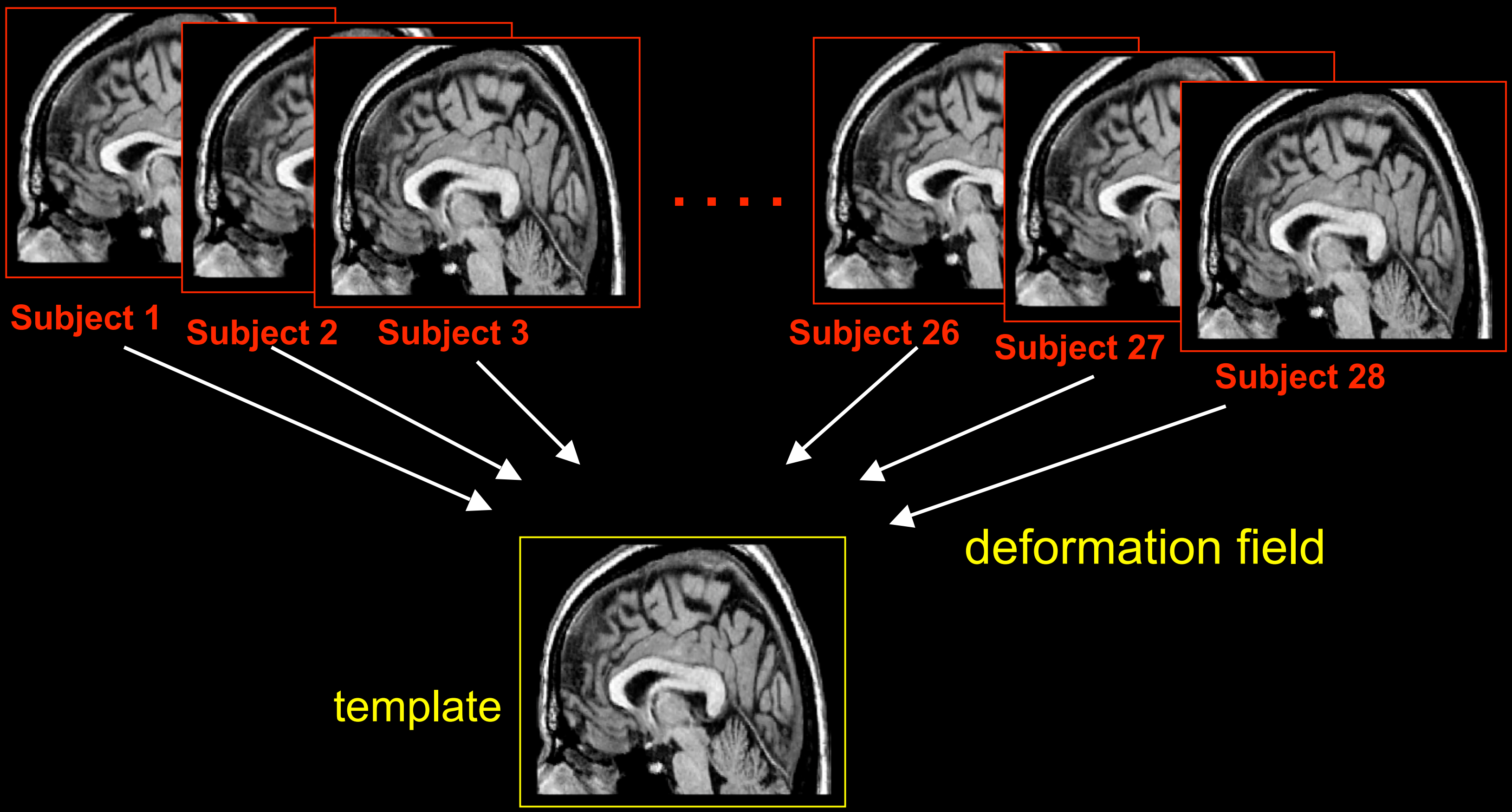

MRIs will be warped into a template and anatomical differences can be compared at a common reference frame.

Why do we need 2D surface normalization?

It can detect subtle surface specific changes better than 3D whole brain volume method.

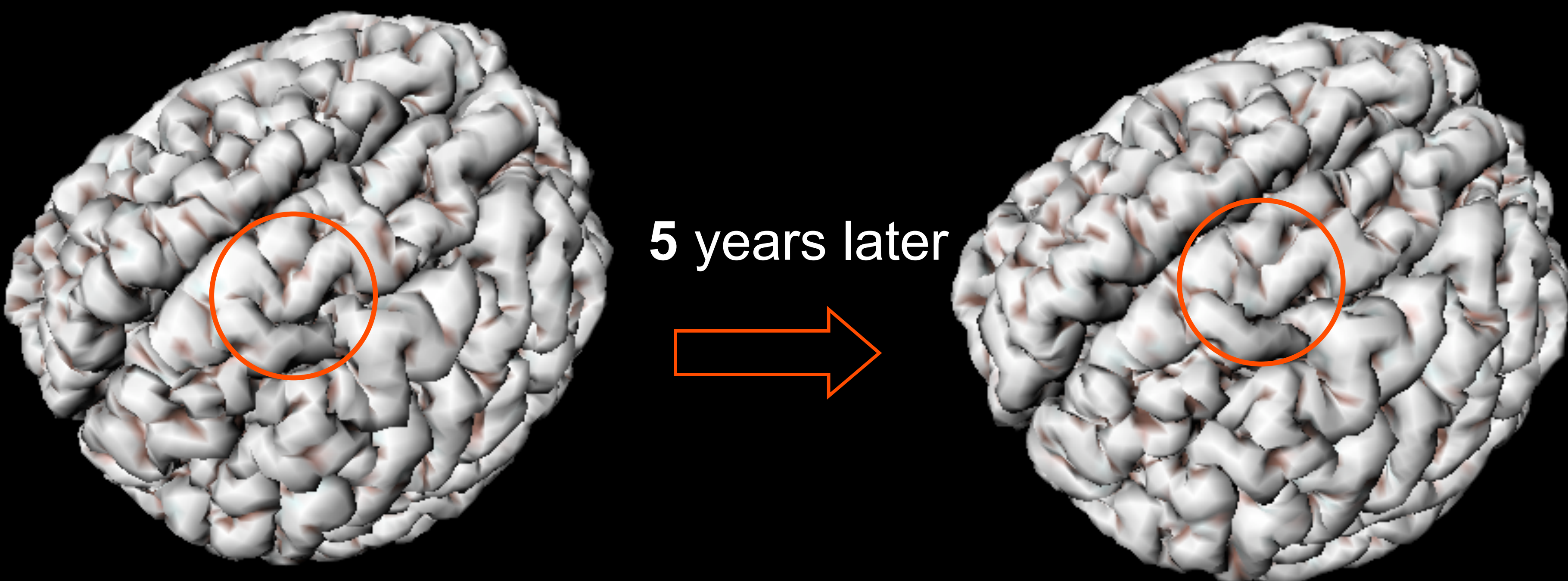

Surface geometry change

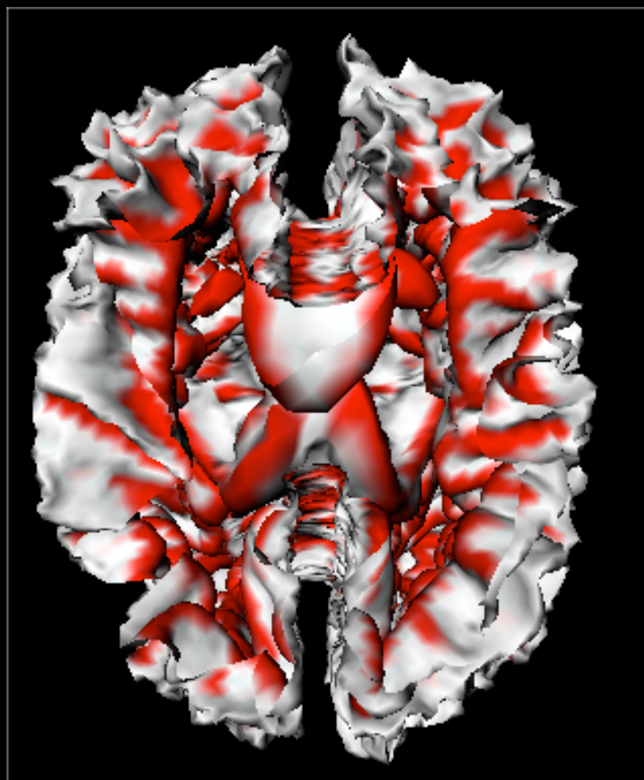

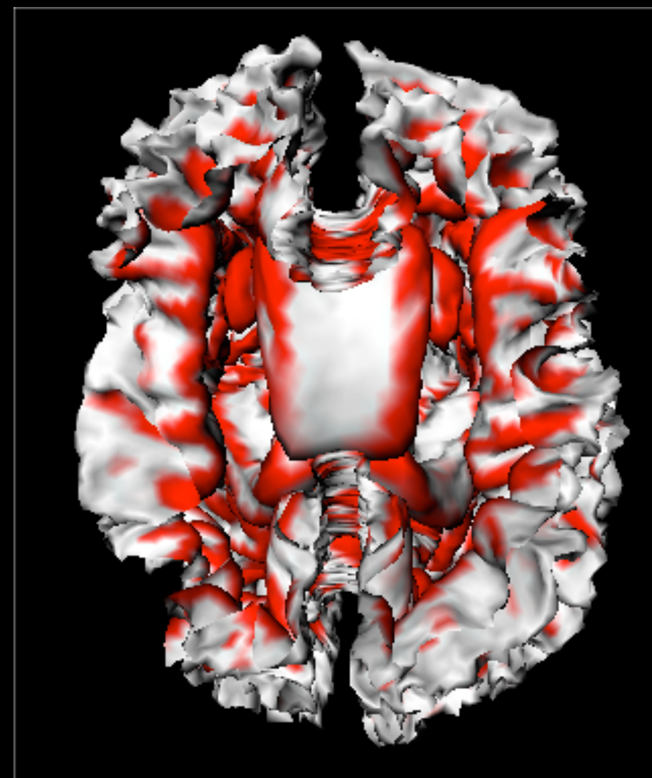

14 year old → 19 year old

Surface Registration

3D whole volume volume registration is insufficient for 2D surface-to-surface matching. 3D volume-to-volume matching tend to cause misalignment of sulci/gyri.

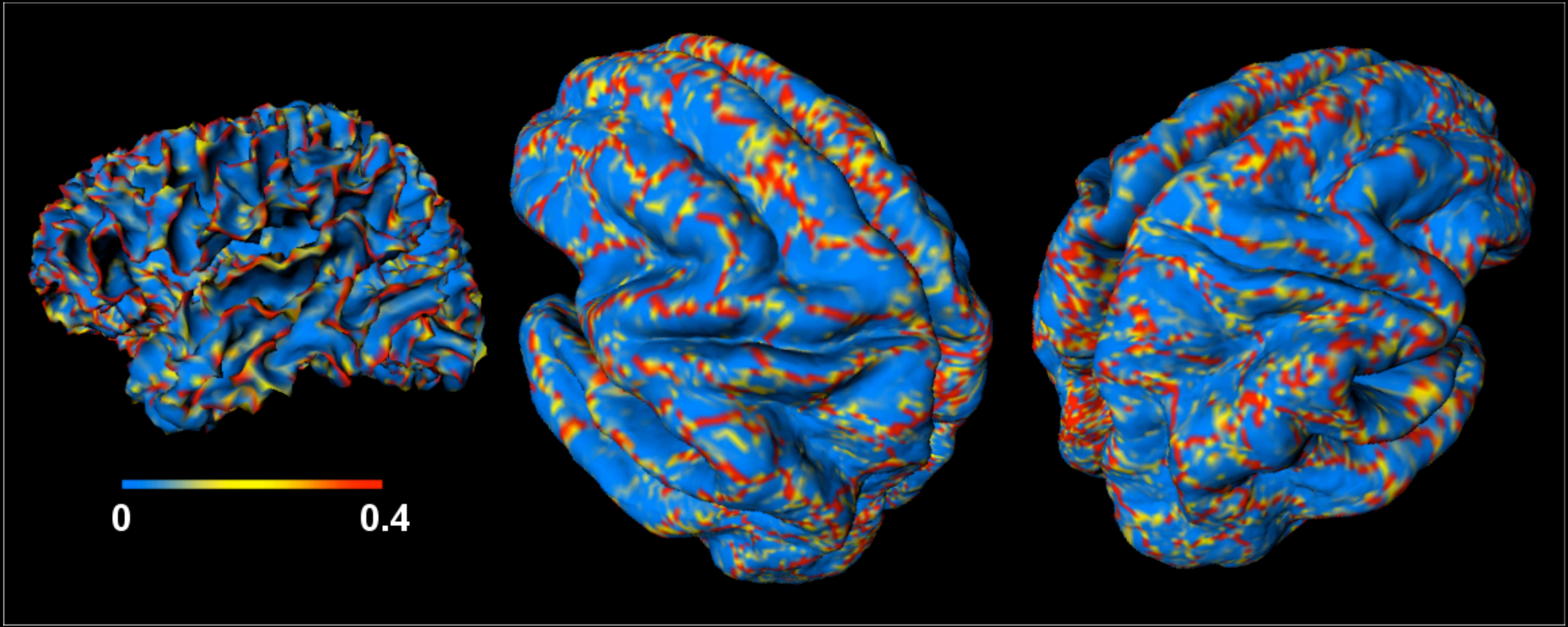

Sum of principal curvature projected onto an average surface template

Sulcal pattern variation within a subject

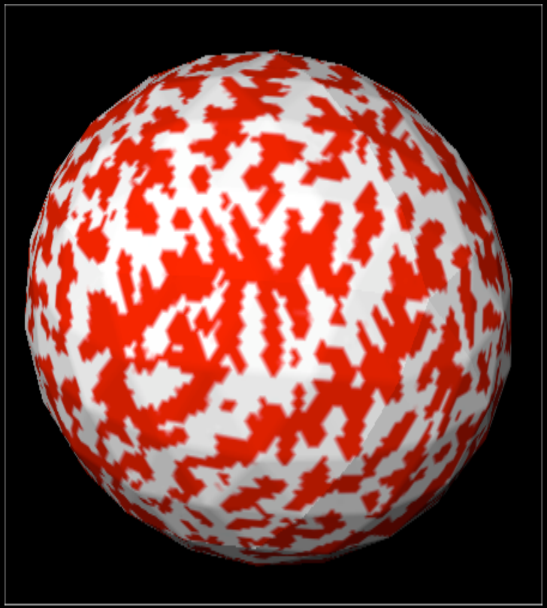

14 year

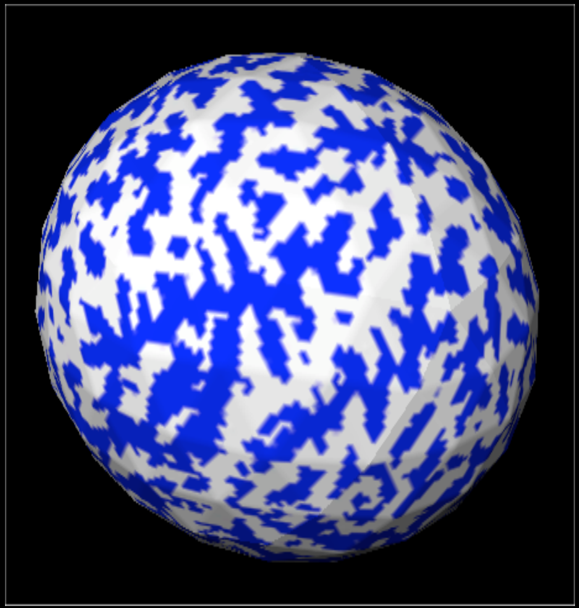

19 year

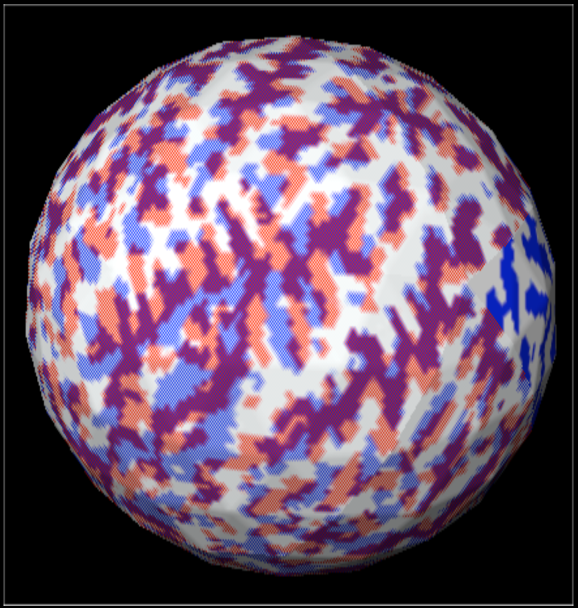

misalignment

Different subjects will have more sulcal variability.

Surface-to-surface registration

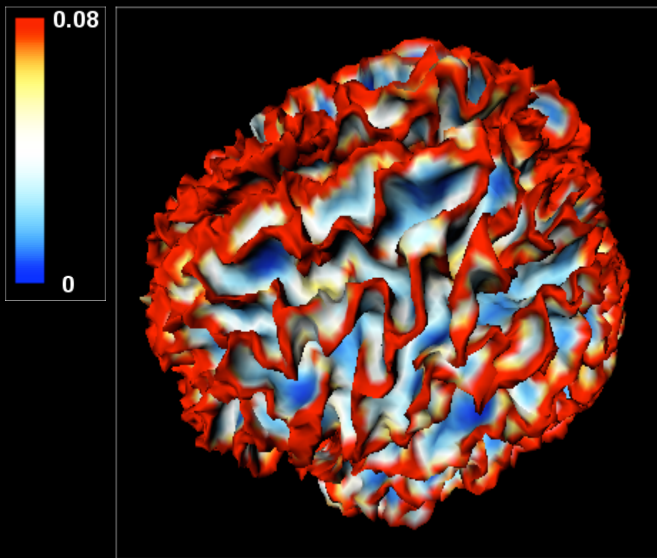

Compute curvatures

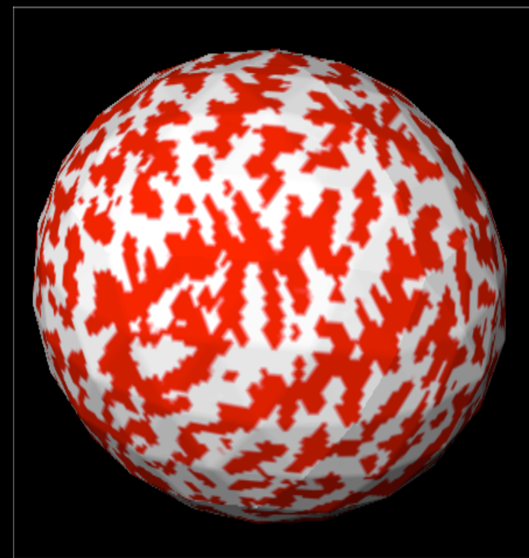

Project onto a sphere

Registration

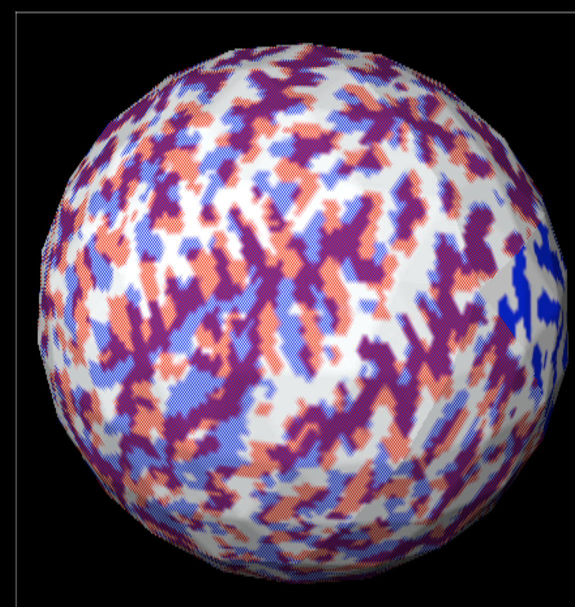

Register a curvature function to another on a unit sphere by maximizing goodness-of-fit and the smoothness of deformation.

Validation of surface registration (149 subjects)

Central & temporal sulci

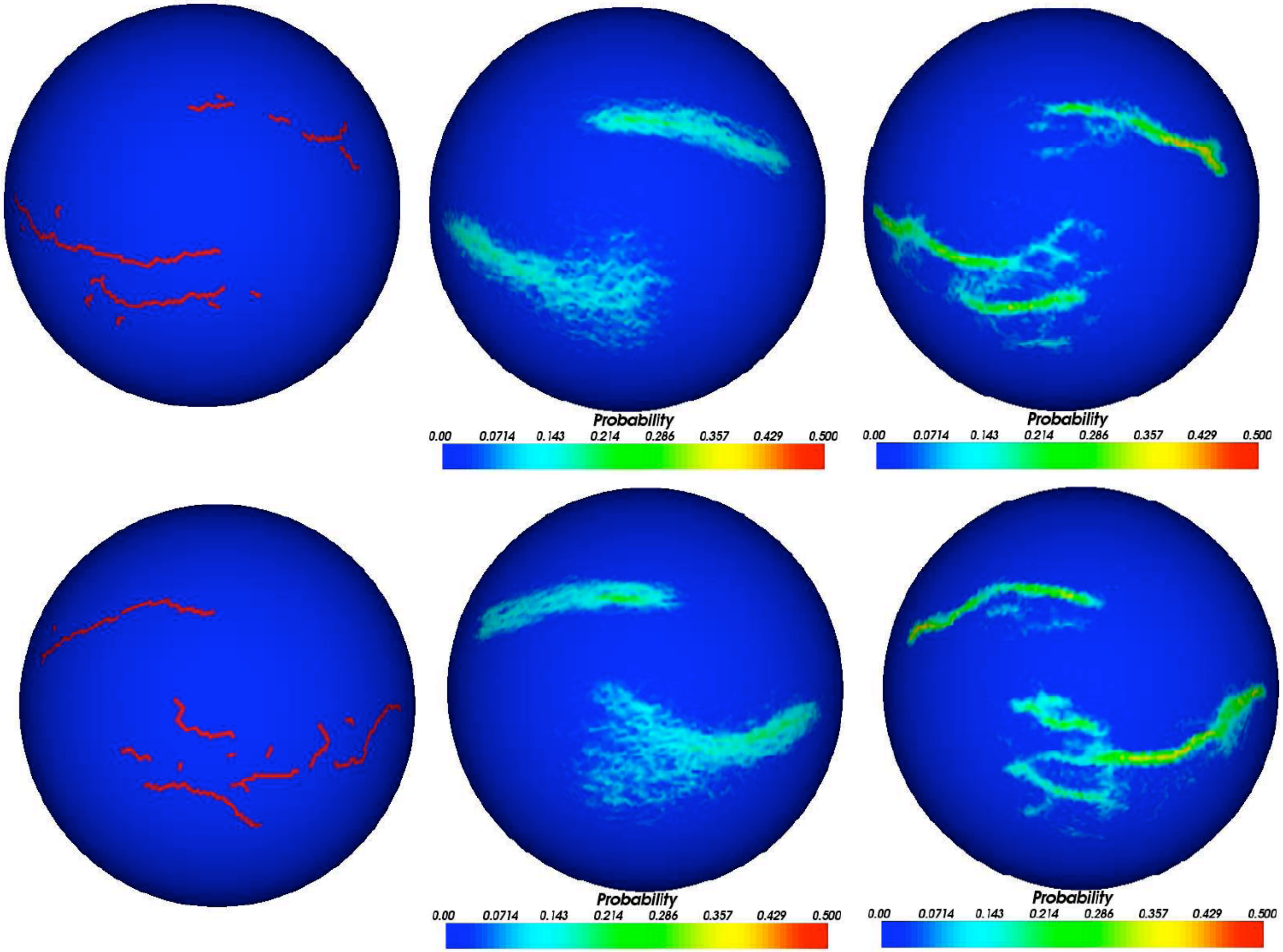

NeuroImage (2005)

Probability of matching in right central sulcus

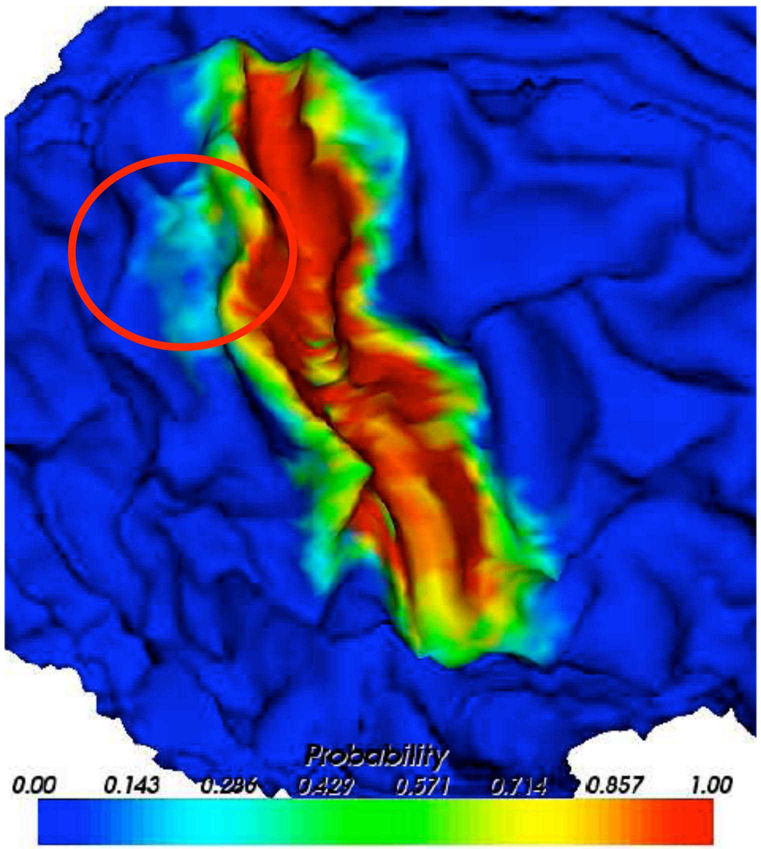

3D volume registration

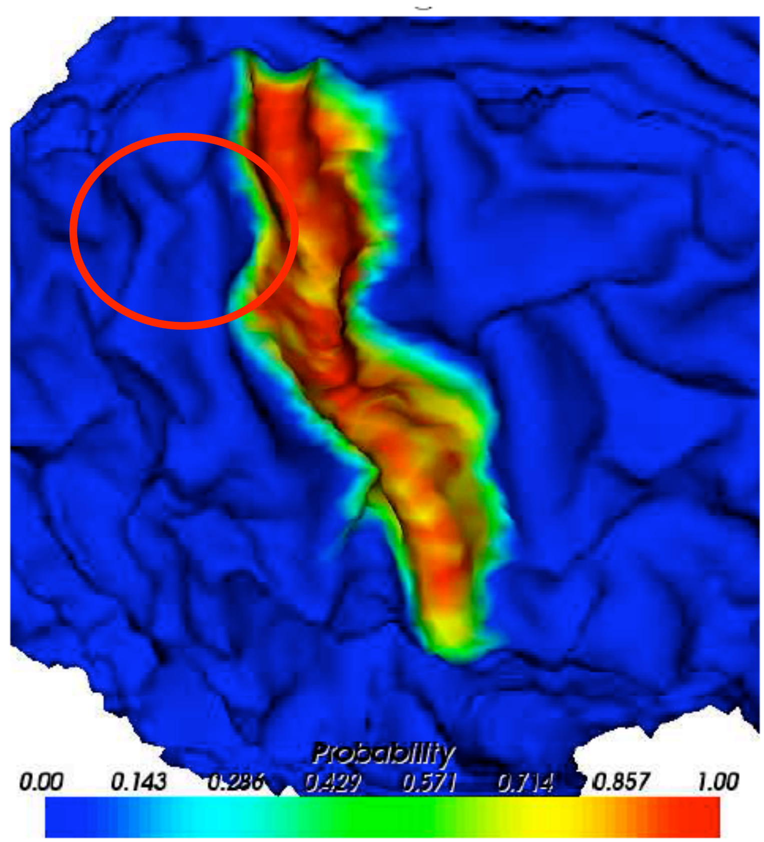

2D surface registration

Trajectory of surface registration

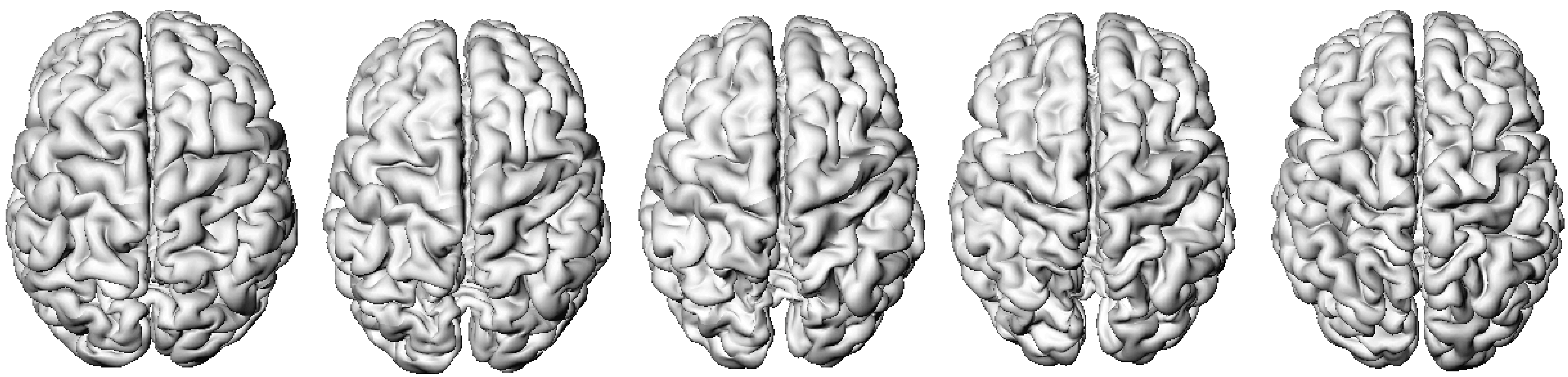

subject 1

subject 2

Based on weighted spherical harmonic representation (TMI, 2007)

Surface Data Smoothing

Why do we smooth data?

- To increase the signal-to-noise ratio (SNR).
- To guarantee the random field theory (RFT) assumption.
- Can correct systematic image processing bias.
- To estimate high order changes (curvatures, metric tensors).

Why Gaussian kernel smoothing?

- Computationally fast.
- Easy numerical implementation
- Performs well.

How to smooth cortical data?

t-statistic map of brain tissue growth before and after smoothing in 28 normal subjects from age 12 to age 16.

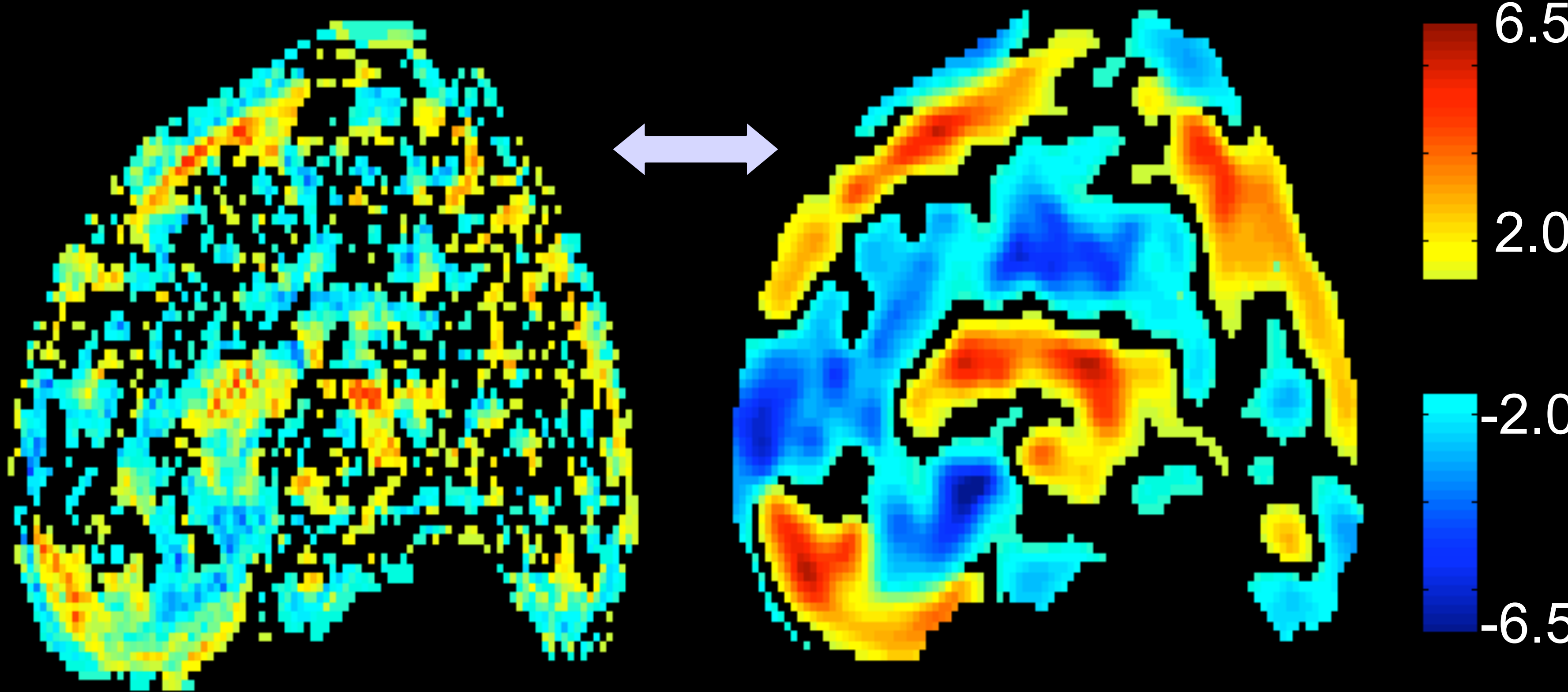

Without smoothing

10mm FWHM Gaussian kernel smoothing

Why Surface-based smoothing ?

1. Increase SNR
2. Increase statistical power
3. Increase localization power
4. Enable tensor computation

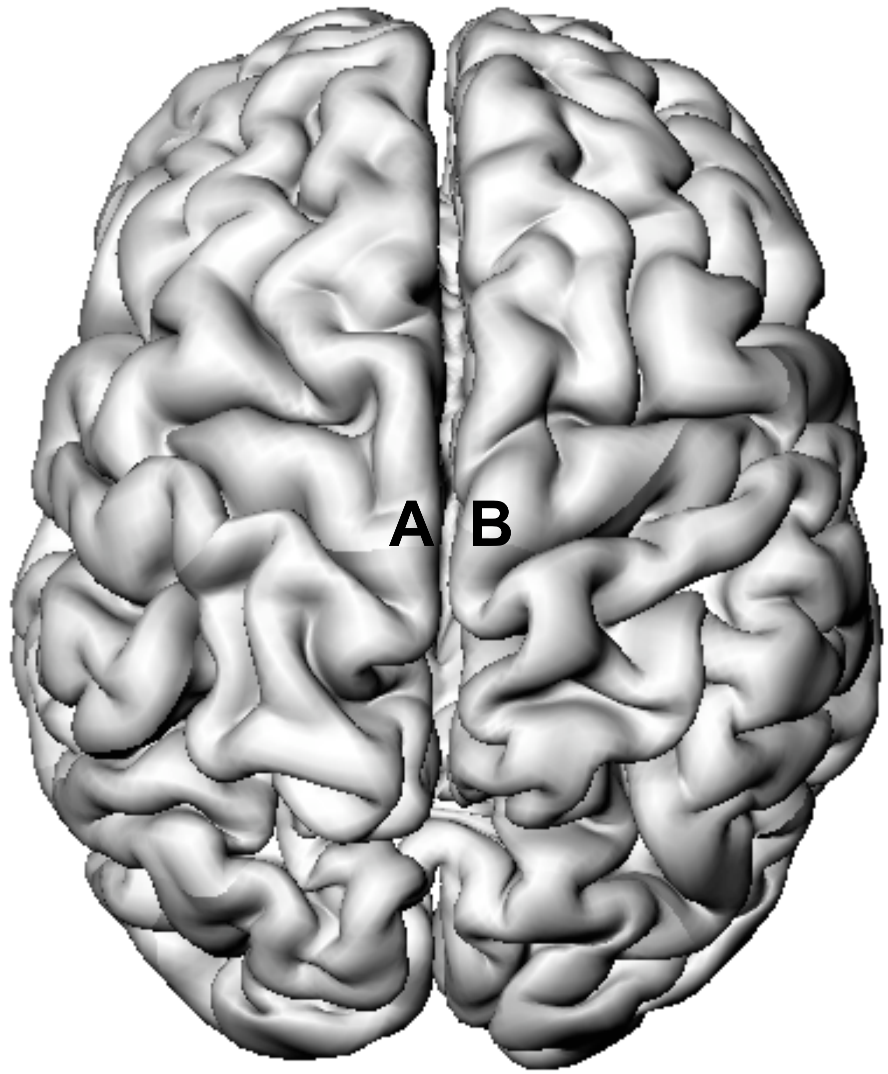

3D Gaussian smoothing will blur data between A and B correlating them spatially while reducing the specificity of detection.

Difficulty of formulating isotropic smoothing

Due to curved geometry, the shortest distance between two points is not a straight line. So we may incorrectly assign less weights to the closer observations.

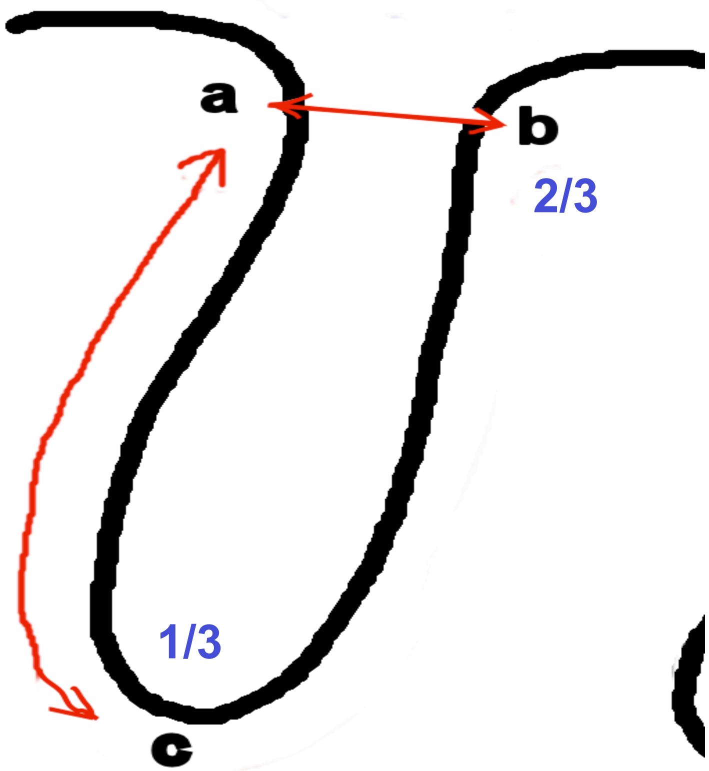

3D volume based weighting

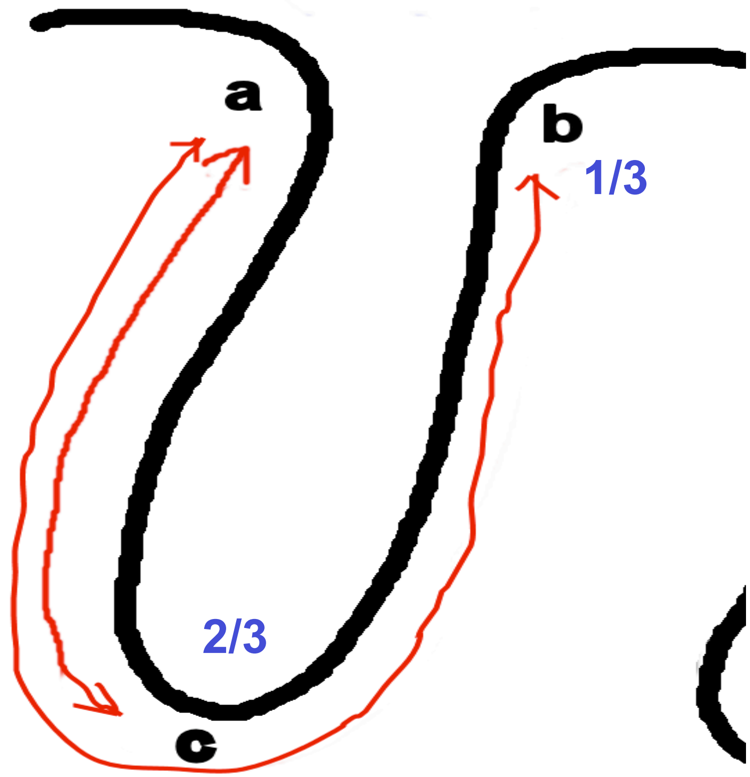

2D surface based weighting

Diffusion smoothing

Smoothing on cortical manifolds can be done by solving an isotropic diffusion equation (NeuroImage, 2003).

5mm FWHM filter size

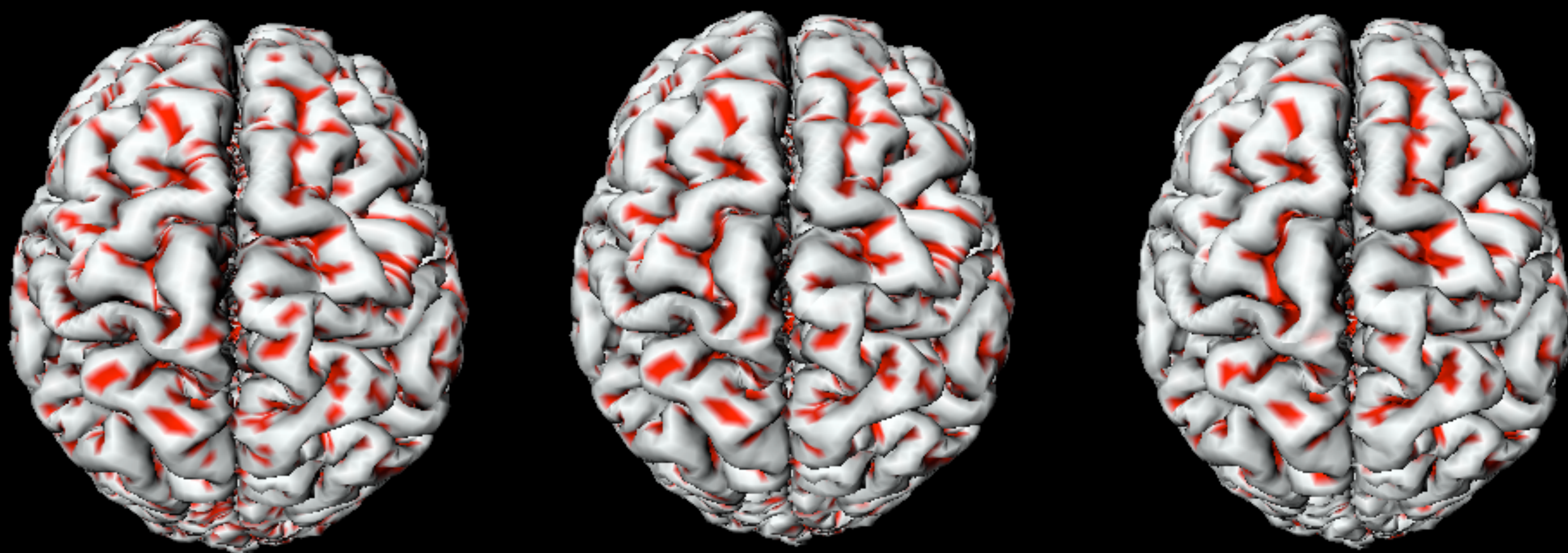

curvature function **20** iterations **100** iterations

Sulcal pattern mapped onto a sphere

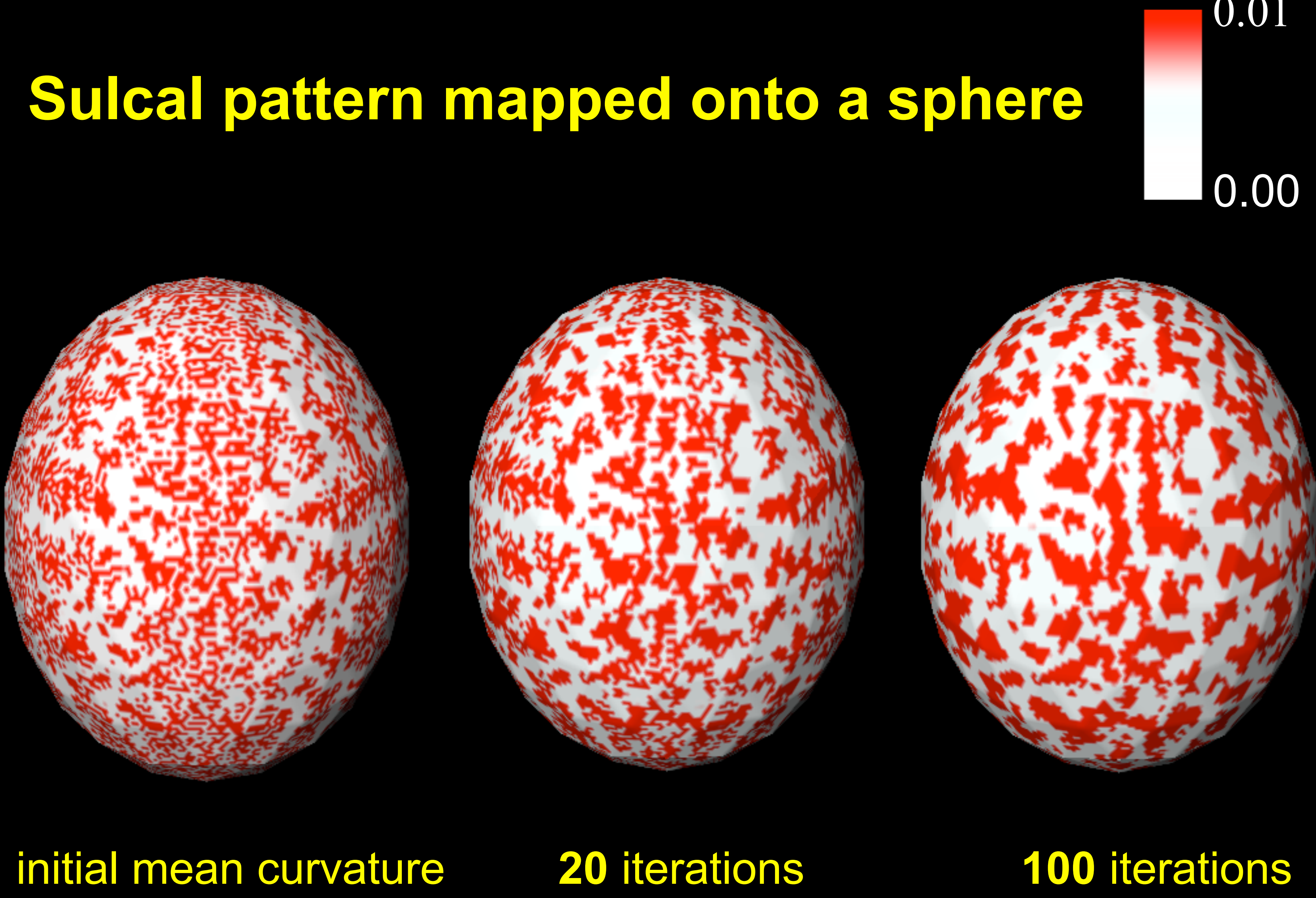

Diffusion smoothing simulation on brain stem

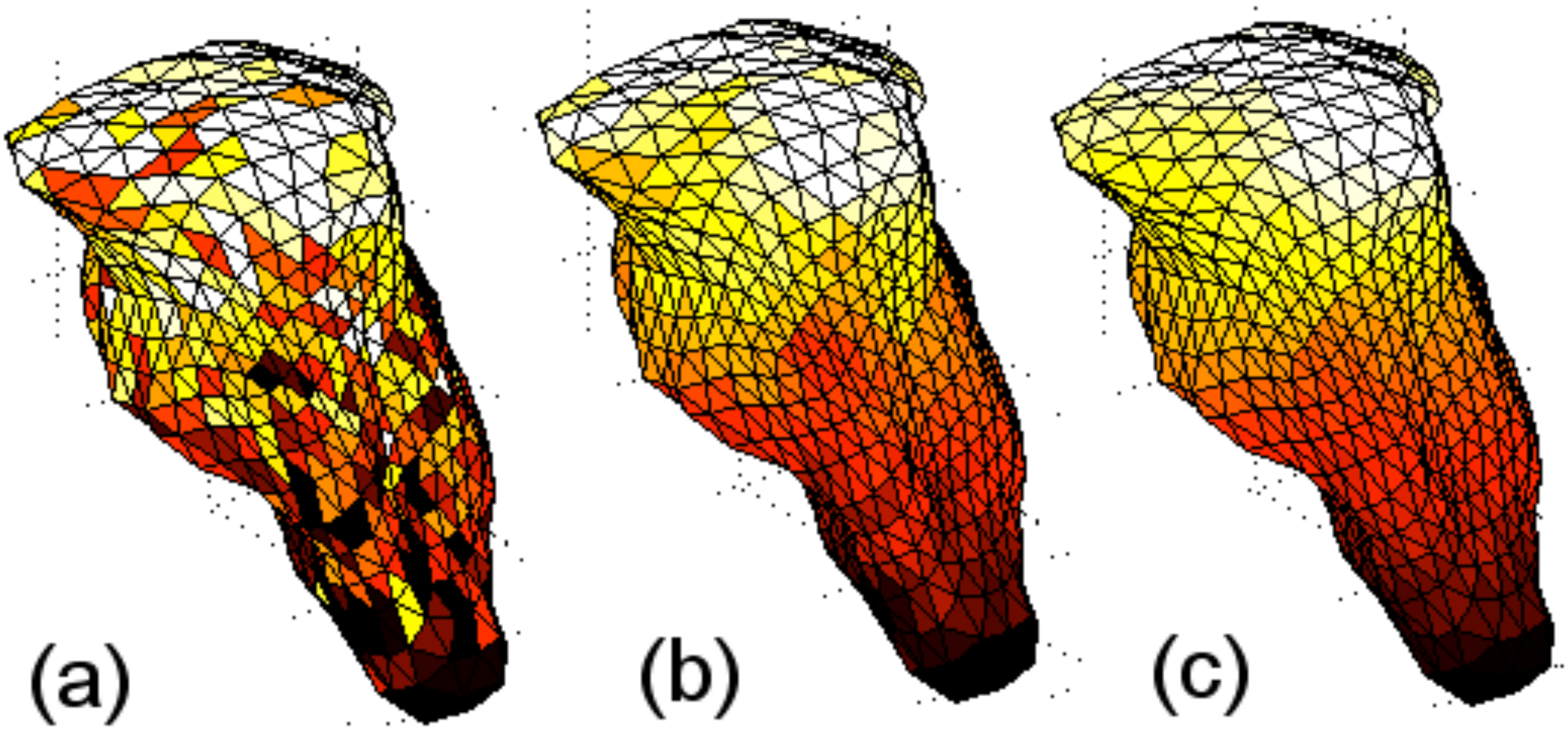

Initial Signal

After 10 iterations

After 20 iterations

Heat kernel smoothing

Iteratively kernel smoothing method (NeuroImage, 2005).

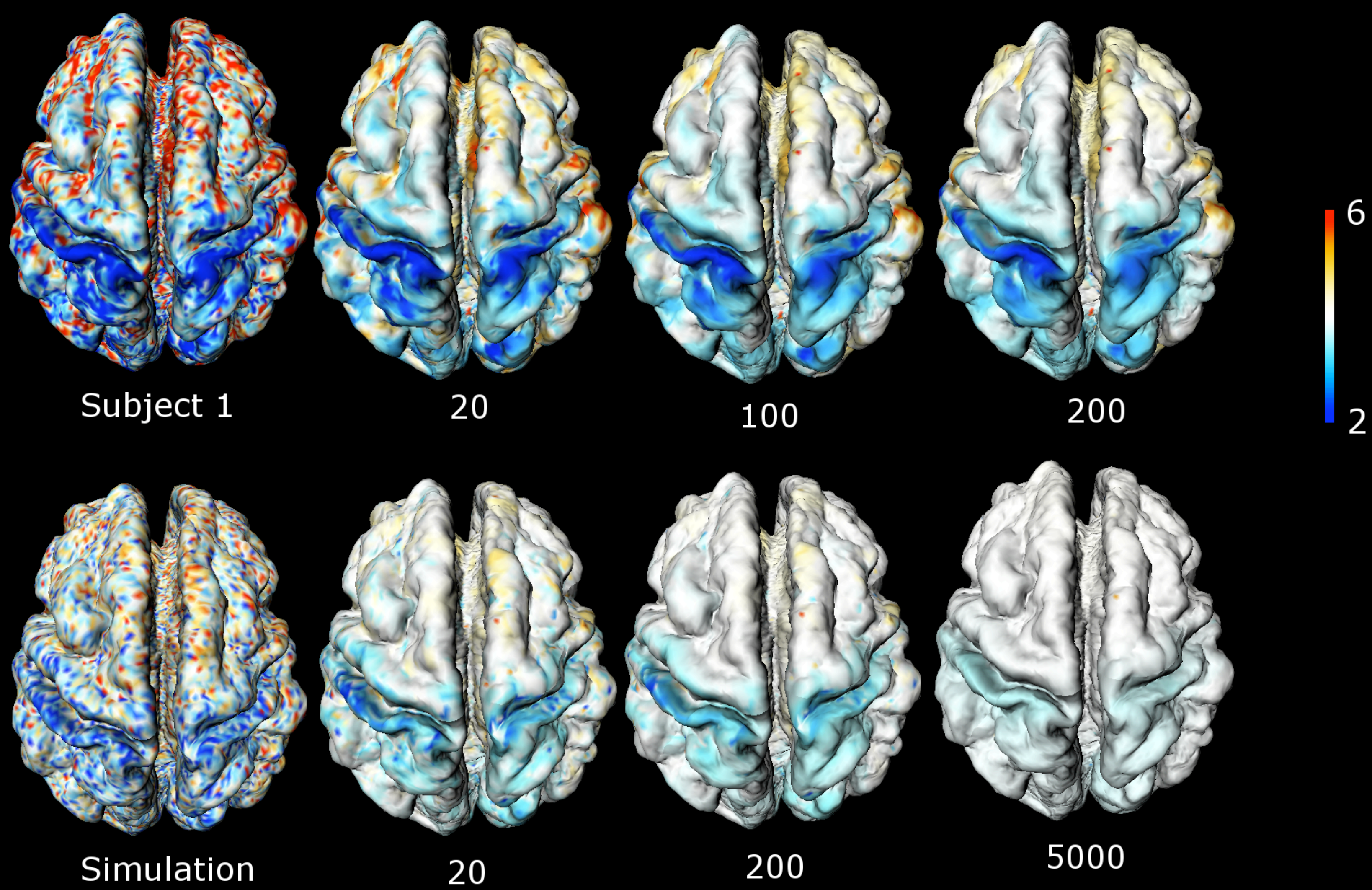

Flat map representation of heat kernel smoothing on cortical thickness

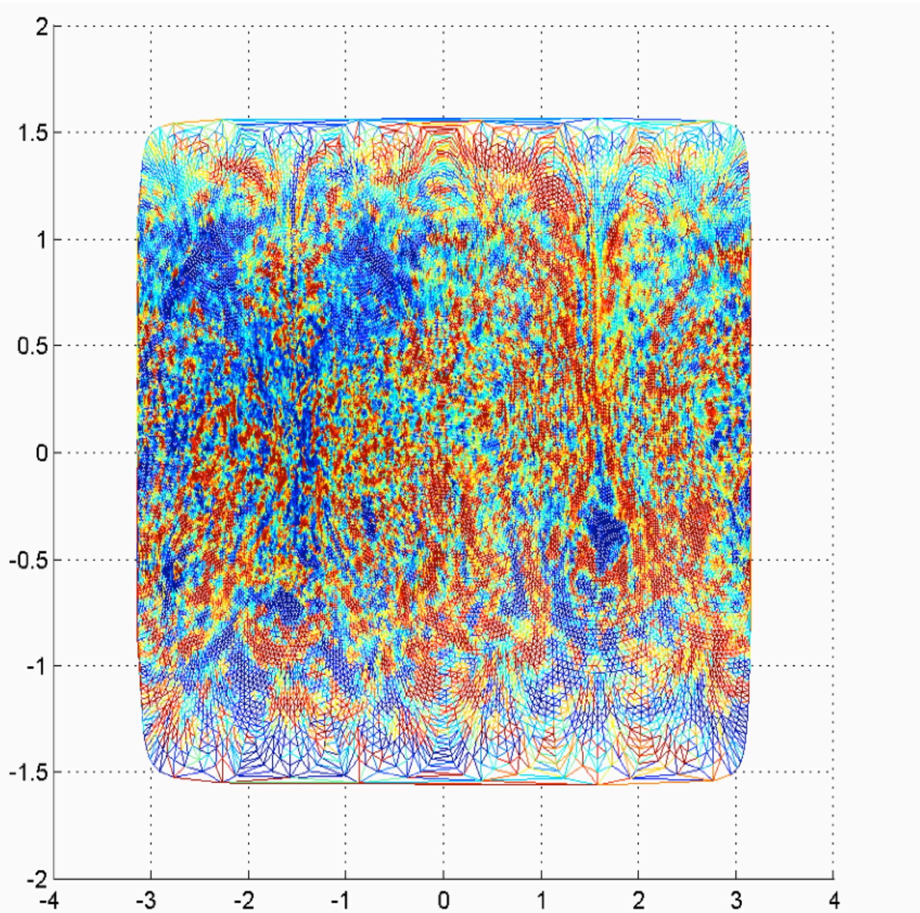

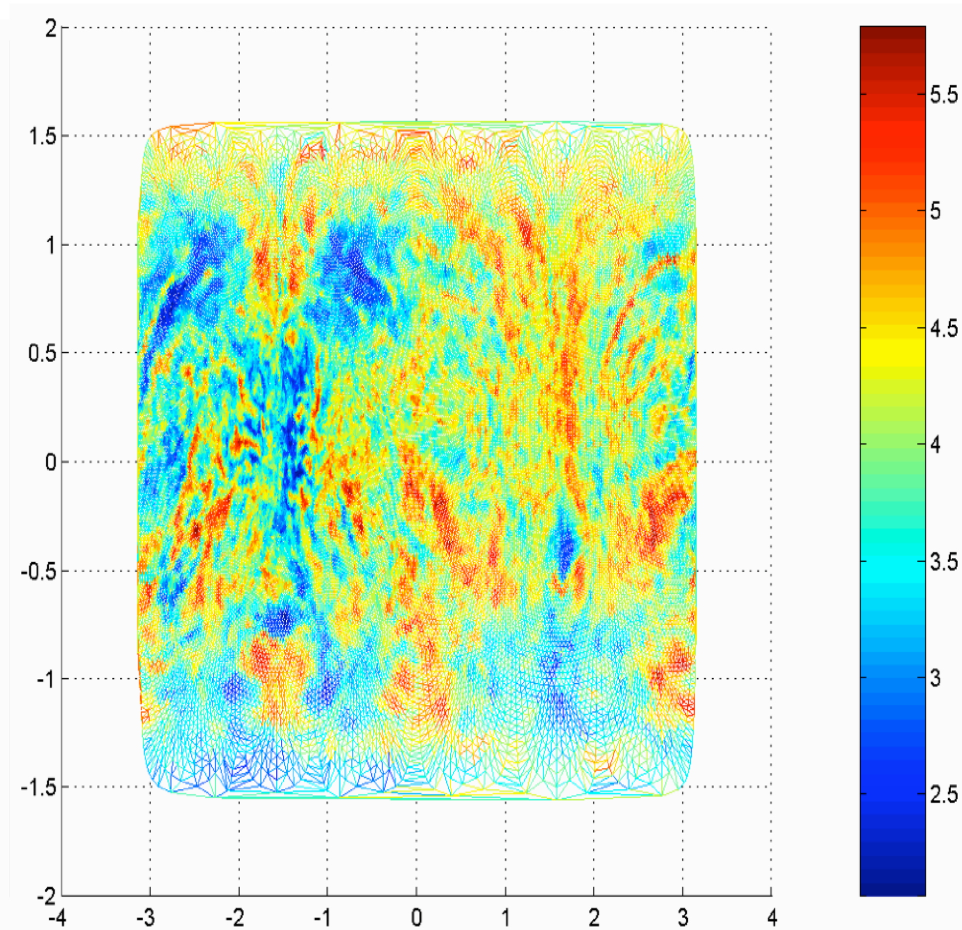

Original data mapped onto a square by cylindrical projection

Heat kernel smoothing

Heat kernel smoothing increases normality of data

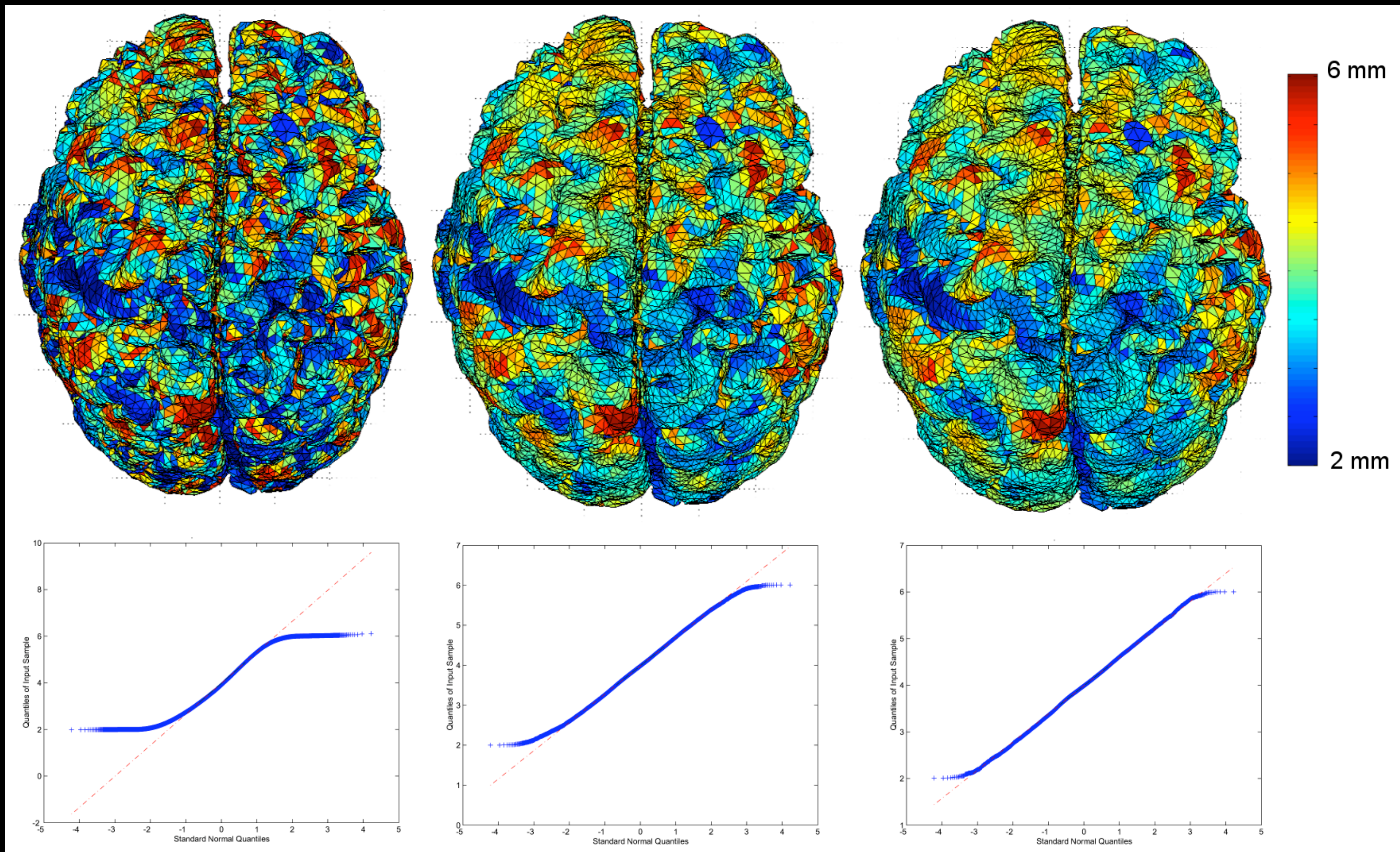

0 iteration   50 iterations   100 iterations

QQ-plot

Multiscale representation of anatomy via weighted-SPHARM

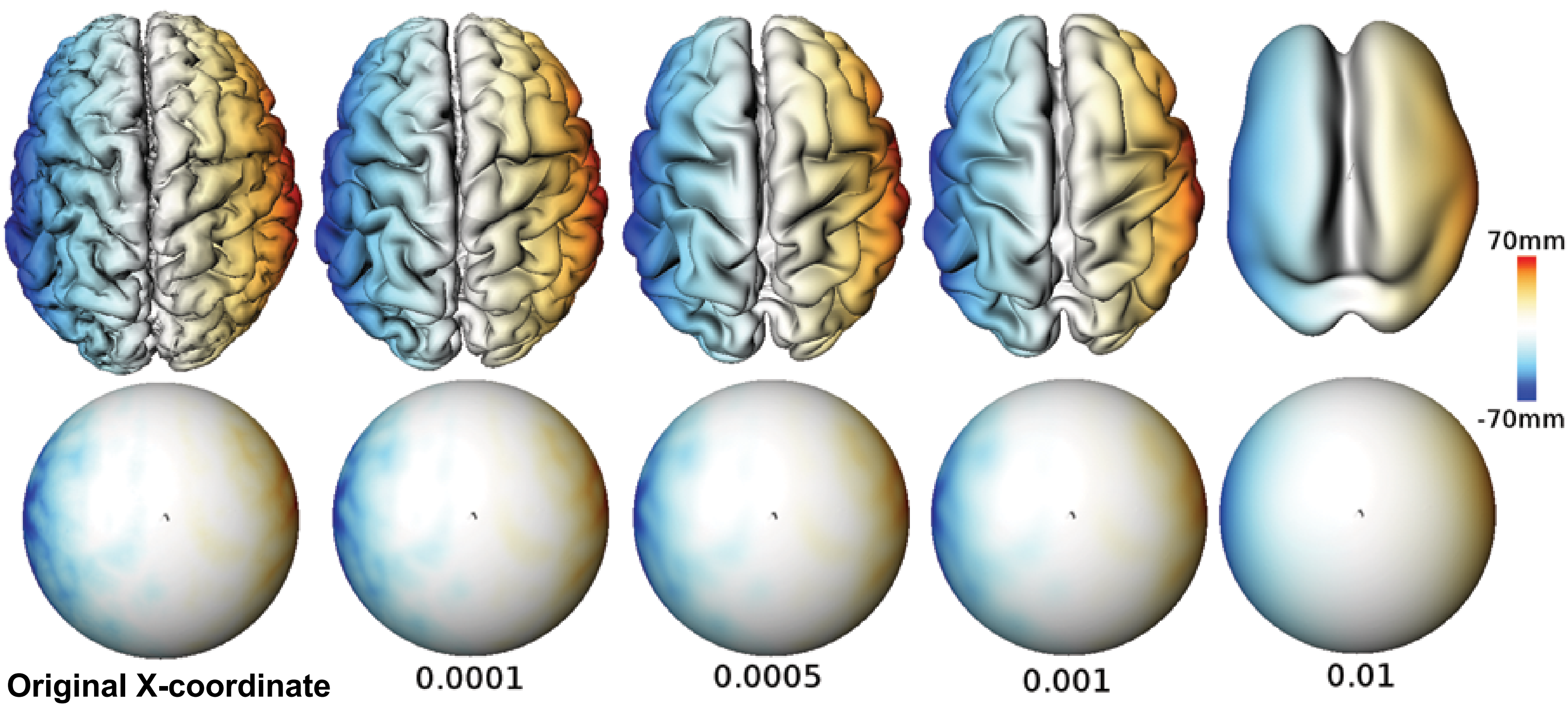

Smoothing of cortical thickness

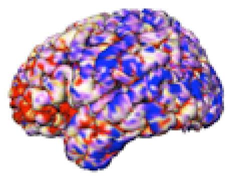

Cortical thickness

1st row: $$\sum_{l=0}^{k} \sum_{m=-l}^{l} e^{-l(l+1)t} \langle f, Y_{lm} \rangle Y_{lm}(\theta, \varphi)$$

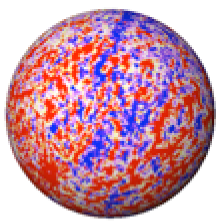

Spherical mapping

2nd row: $$\sum_{m=-k}^{k} e^{-l(l+1)t} \langle f, Y_{lm} \rangle Y_{lm}(\theta, \varphi)$$

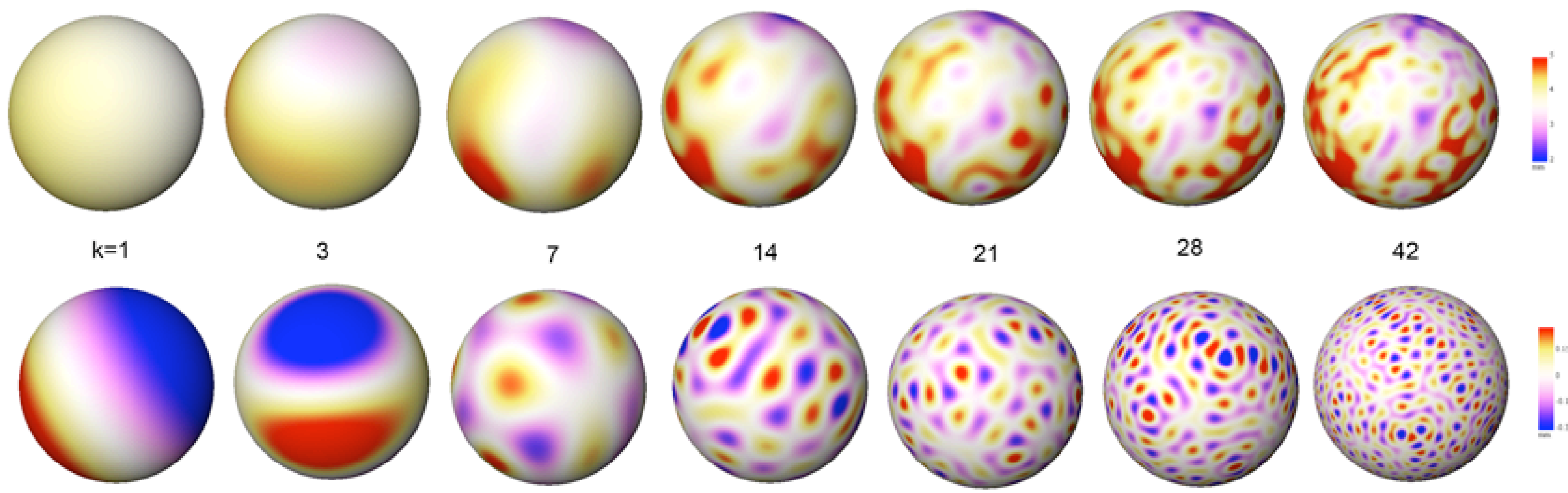

Statistical Analysis

Multiple comparisons

$$\boxed{H_0 : \theta_1(p) = \theta_2(p) \text{ for all } p \in \partial\Omega}$$

v.s.

$$H_1 : \theta_1(p) > \theta_2(p) \text{ for some } p \in \partial\Omega.$$

The above hull hypothesis is the intersection of collection of hypothesis

$$\boxed{H_0 = \bigcap_{p \in \partial\Omega} H_0(p)}$$

Type I error

$$\begin{aligned}
\alpha &= P(\text{ reject at least one } H_0(p) | H_0 \text{ true }) \\
&= P\Big(\bigcup_{p \in \partial\Omega} \{T(p) > h\}\Big) \\
&= 1 - P\Big(\bigcap_{p \in \partial\Omega} T(p) \le h\}\Big) \\
&= 1 - P(\sup_{p \in \partial\Omega} T(p) \le h) \\
&= \boxed{P(\sup_{p \in \partial\Omega} T(p) > h).}
\end{aligned}$$

***t* random field**

Excursion Probability

$Z(x)$: Stationary isotropic random field in $x \in \Omega \subset \mathbb{R}^N$

$A_z = \{x : Z(x) > z\}$ excursion set

$\chi(A_z)$: Euler characteristic

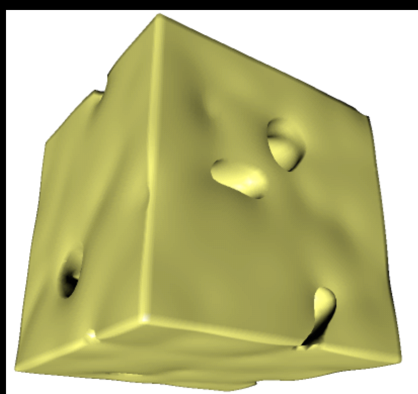

z = -10

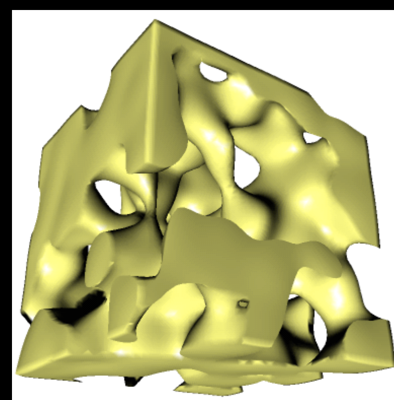

z = 0

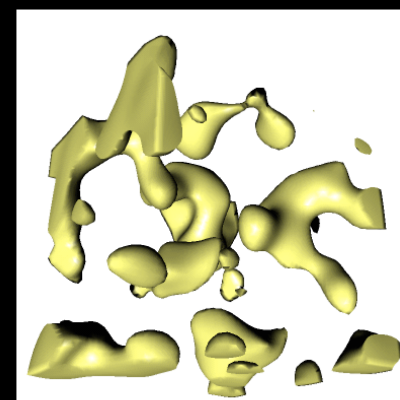

z = 10

$$\boxed{P\left(\max_{x\in\Omega} Z(x) > z\right) \approx \mathbb{E}\left(\chi(A_z)\right)}$$

(Adler, 1984)

T random field on manifolds

$$P\Big(\max_{\mathbf{x}\in\partial\Omega_{atlas}} T(\mathbf{x}) \geq y\Big) \approx 2\rho_0(y) + \|\partial\Omega_{atlas}\|\rho_2(y)$$

Euler characteristic density

$$\rho_0(y) = \int_y^\infty \frac{\Gamma(\frac{n}{2})}{((n-1)\pi)^{1/2}\Gamma(\frac{n-1}{2})}\Big(1+\frac{y^2}{n-1}\Big)^{-n/2} dy,$$

$$\rho_2(y) = \frac{1}{\mathrm{FWHM}^2}\frac{4\ln 2}{(2\pi)^{3/2}}\frac{\Gamma(\frac{n}{2})}{(\frac{n-1}{2})^{1/2}\Gamma(\frac{n-1}{2})}y\Big(1+\frac{y^2}{n-1}\Big)^{-(n-2)/2}$$

Worsley (1995, NeuroImage)

corrected *p*-value map for *t* test

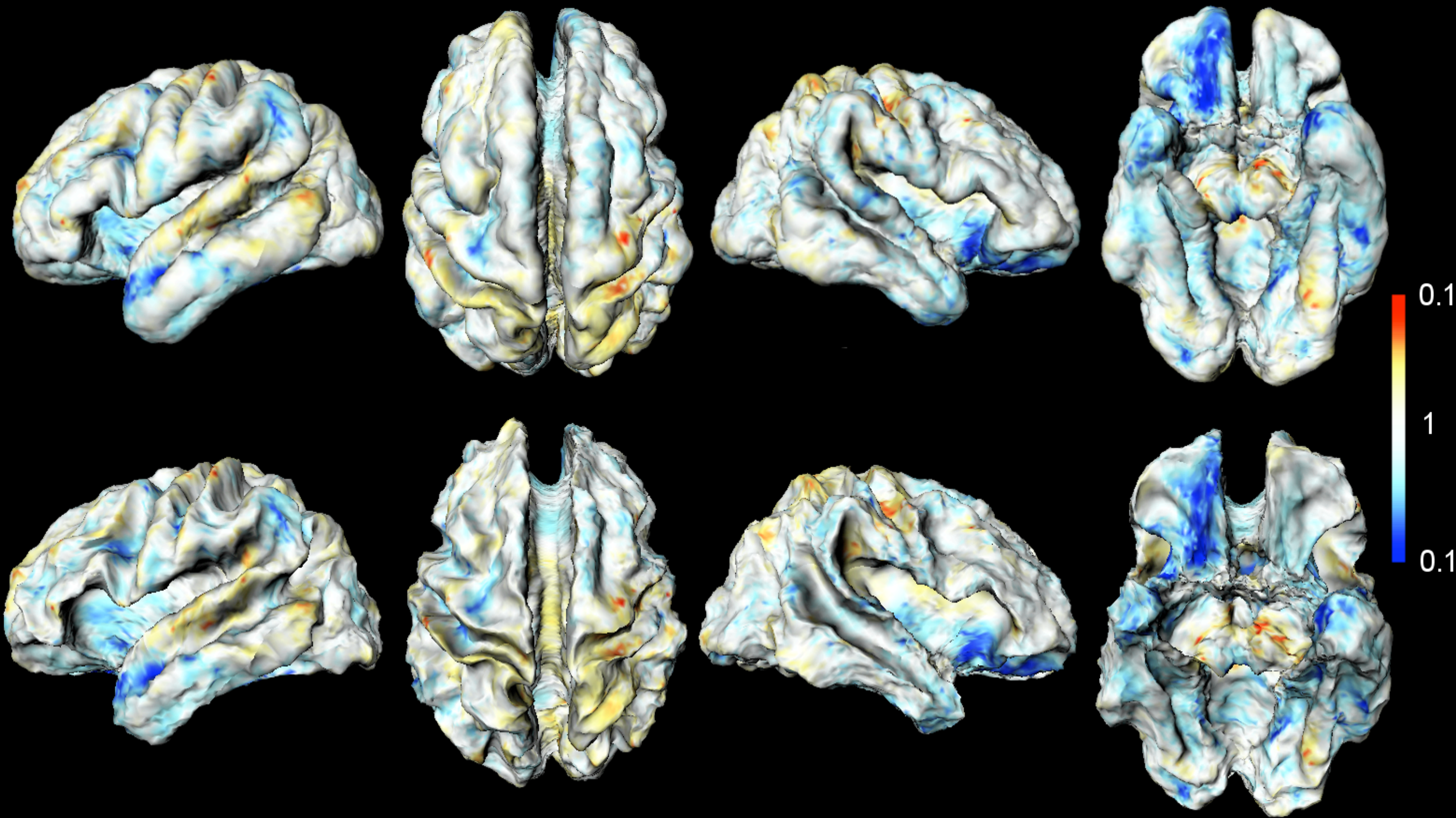

Decrease: left superior temporal sulcus, left occipital-temporal gyrus, right orbital prefrontal

Increase: left superior temporal gyrus, left middle temporal gyrus, left and right postcentral sulci

corrected *p*-value map for *F* test correcting for age

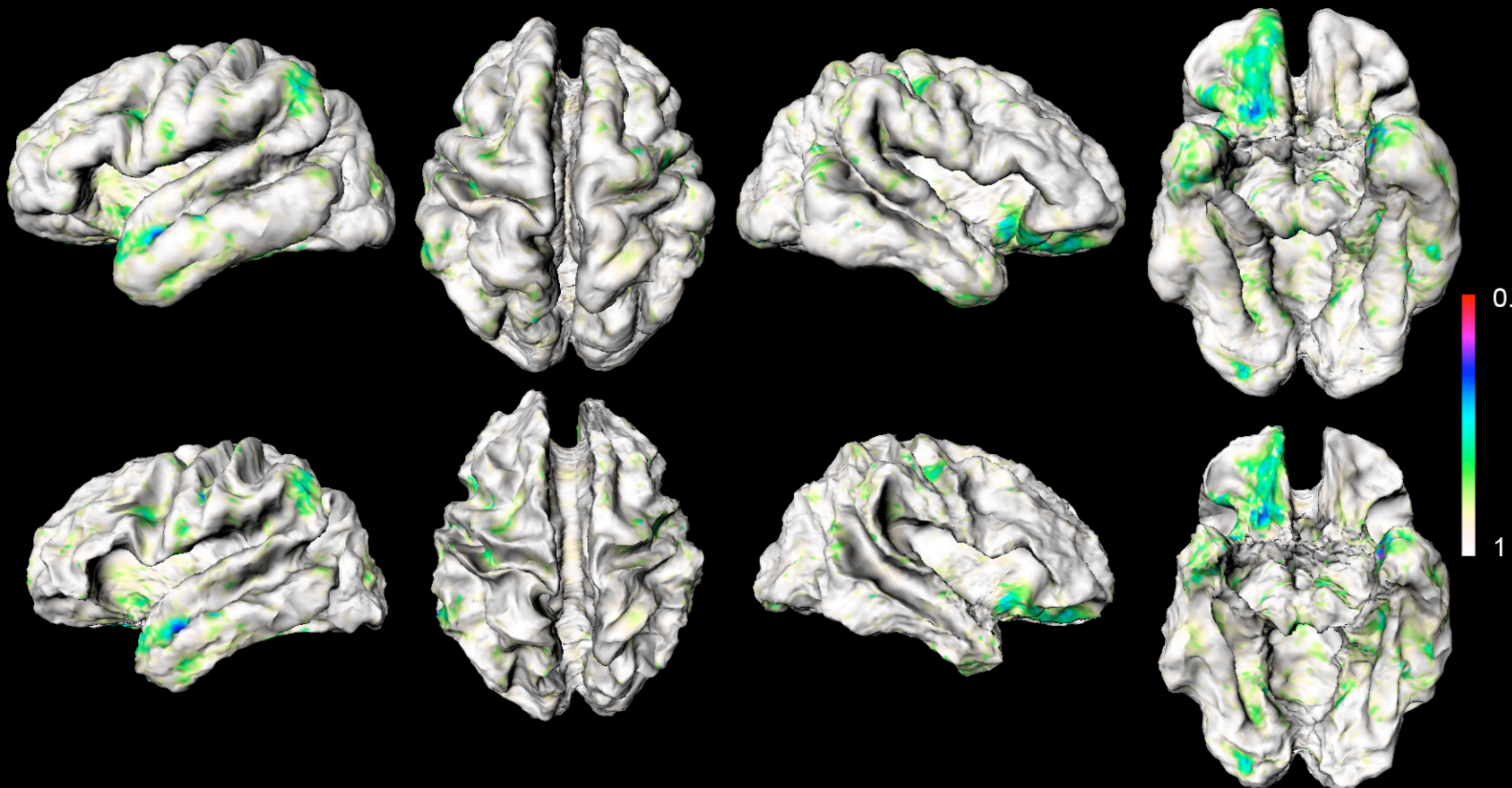

Decrease: left superior temporal sulcus
left occipital-temporal gyrus
right orbital prefrontal

Additional Analysis

Brain-Behavior Correlation

Facial emotion discrimination task response time

24 emotional faces, 16 neutral faces

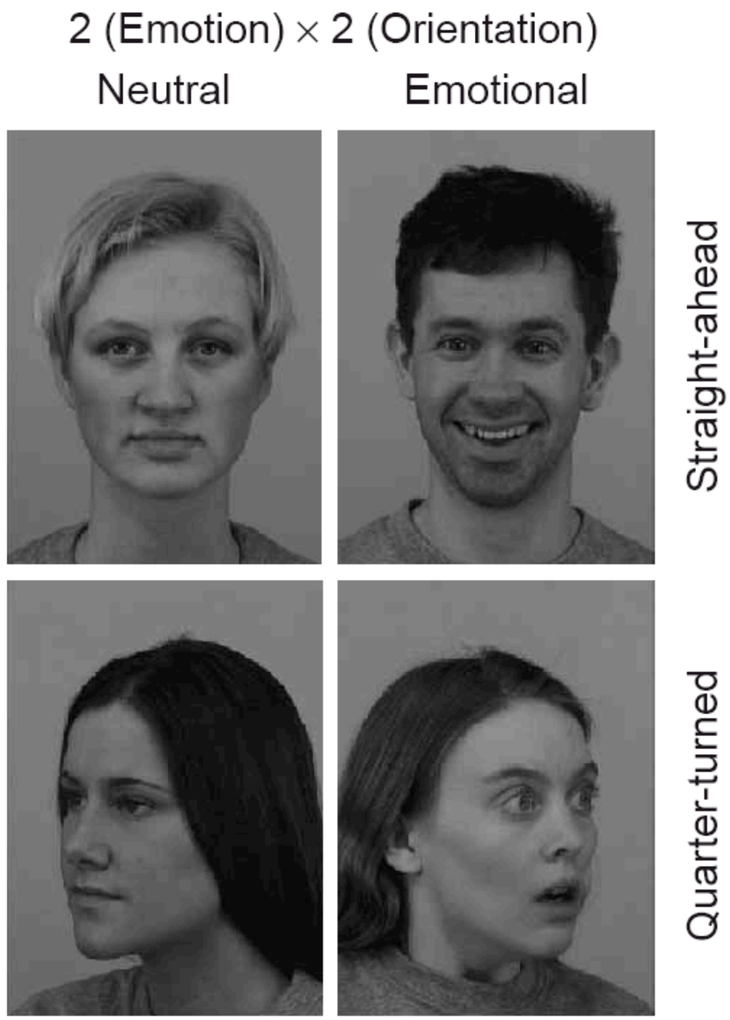

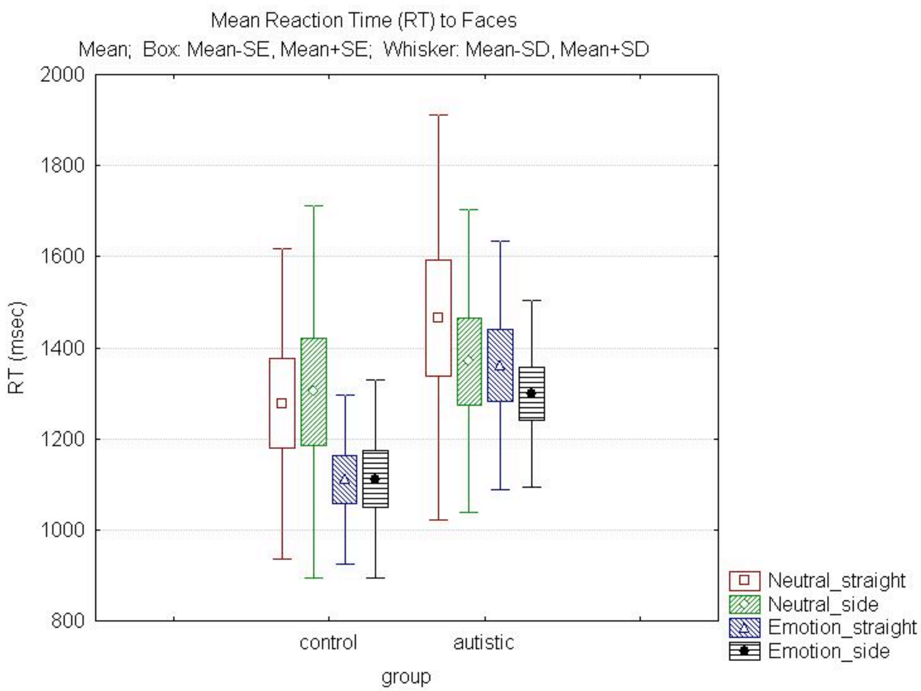

Dalton et al. (Nature Neuroscience 2005)

Correlating thickness and behavioral measure

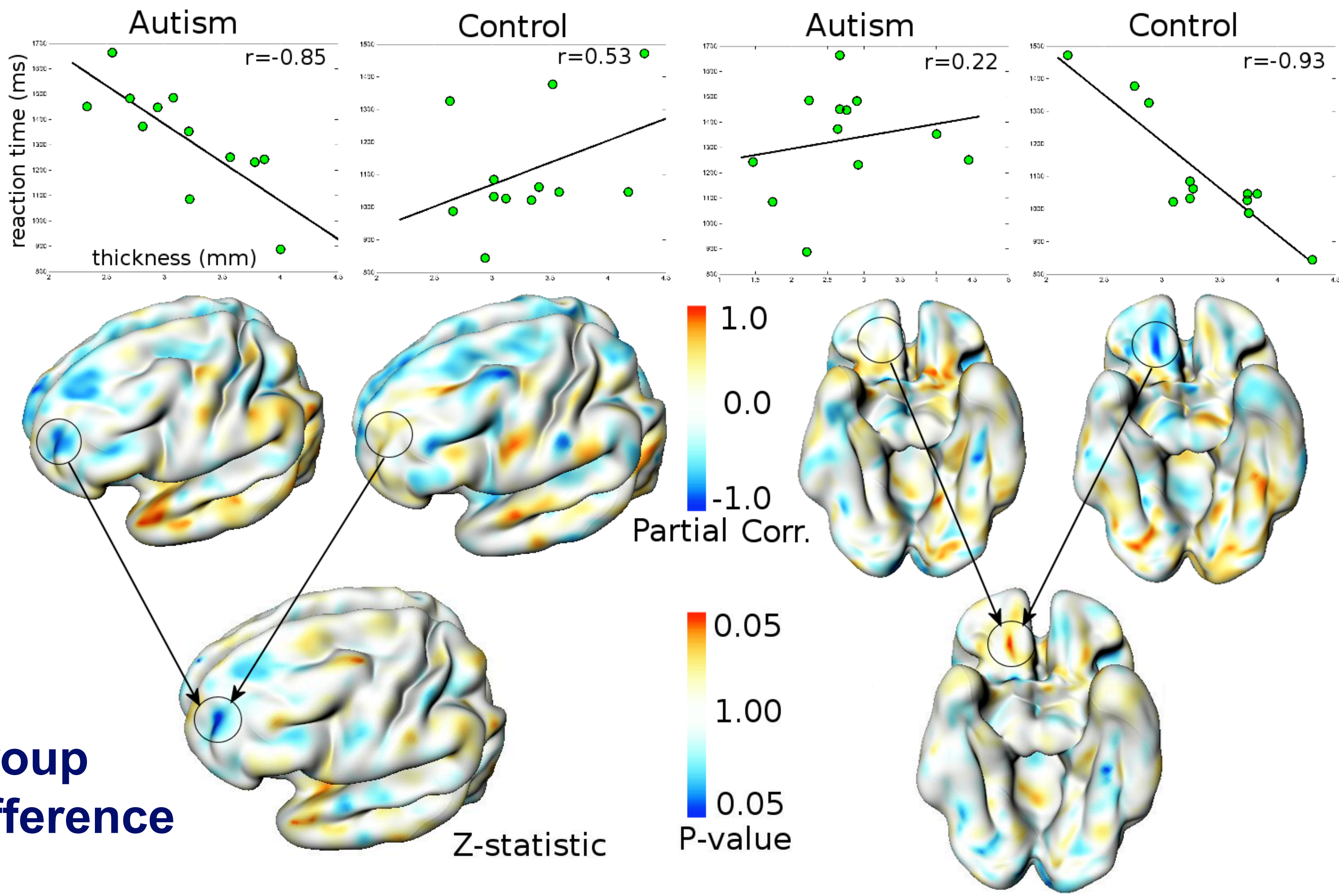

Group difference

Correlation difference between the groups.

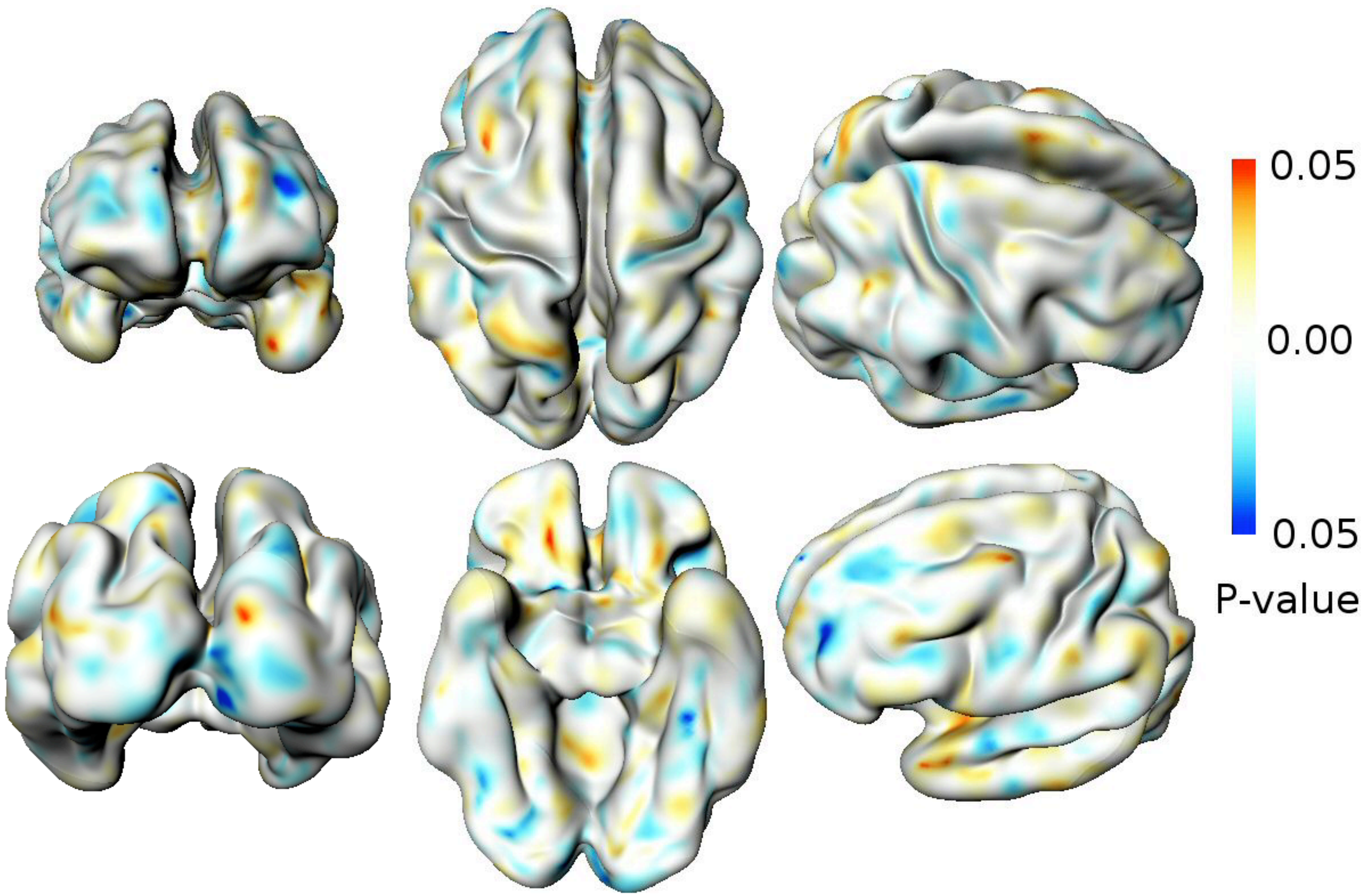

Brain substructure modeling

SPHARM representation of hippocampus

Overfitting

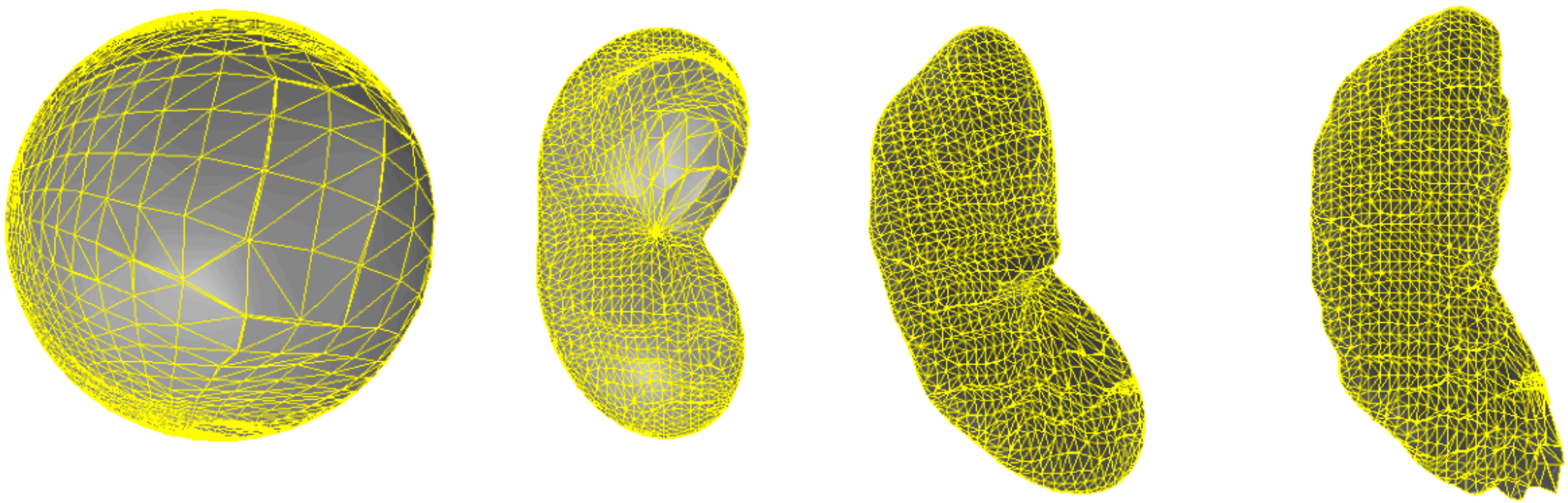

degree 1 degree 5 degree 10 degree 50

Optimal representation

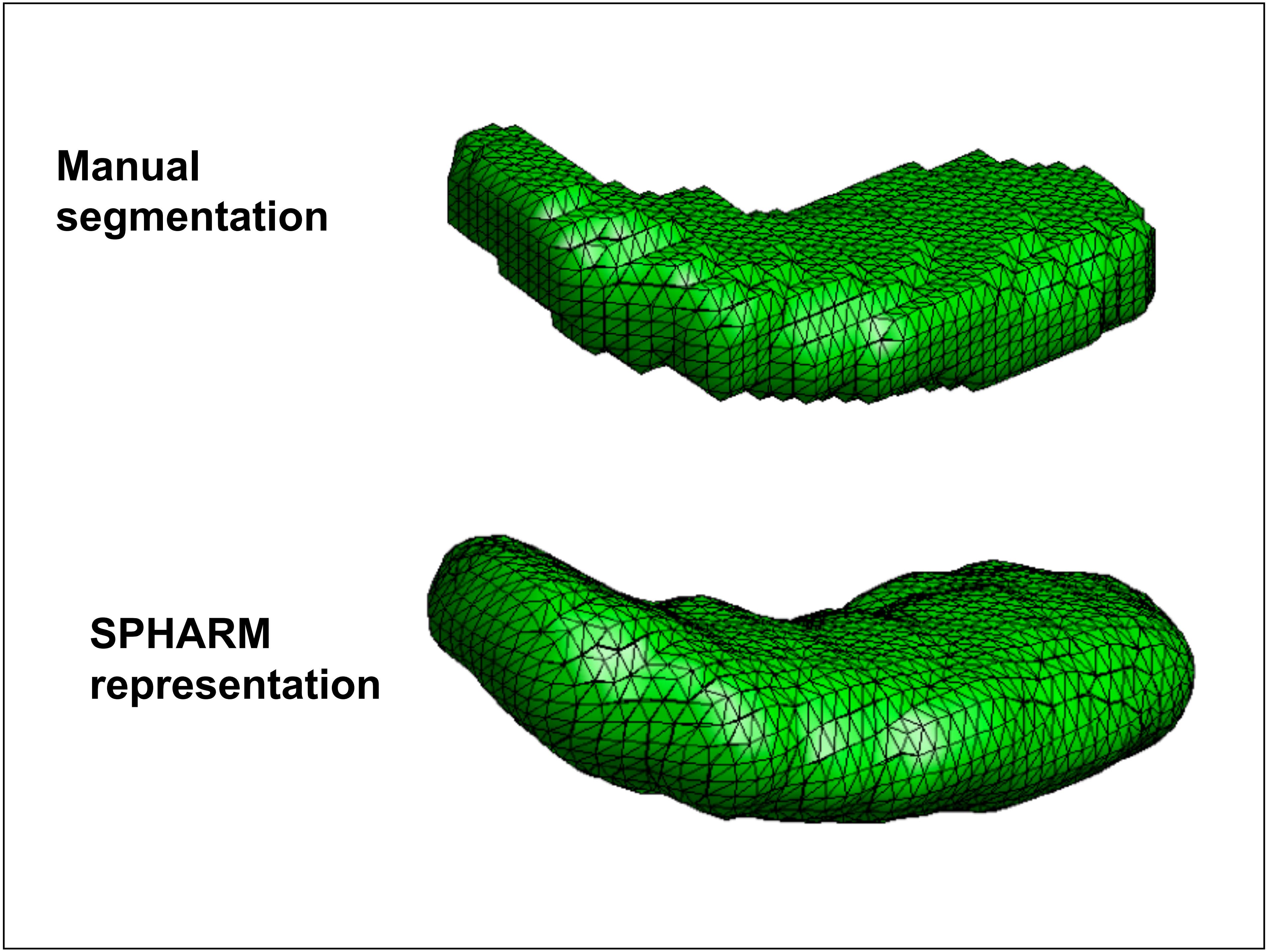
Manual
segmentation
SPHARM
representation

Corpus callosum modeling

The segmentation results of corpus callosum

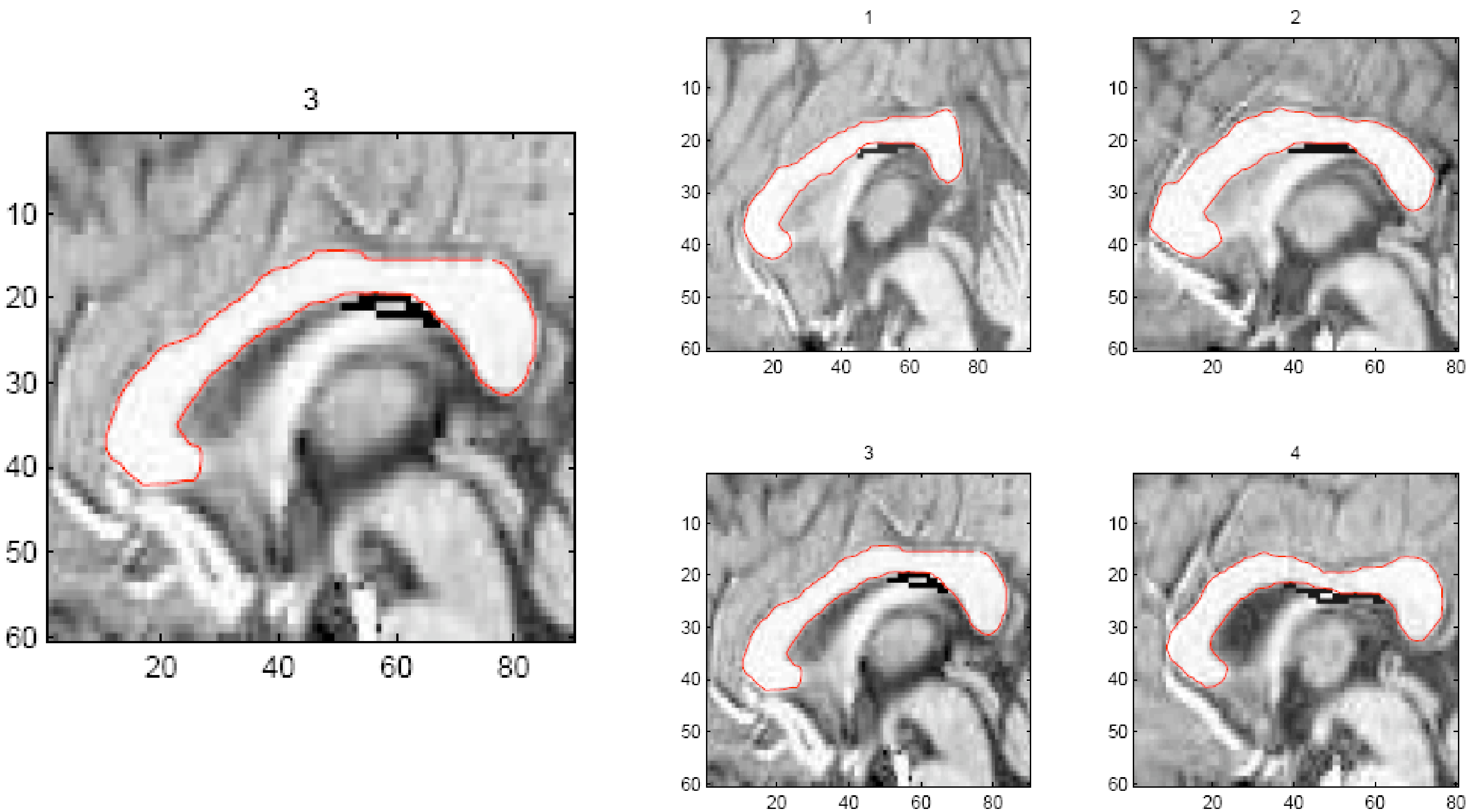

Parametric modeling of corpus callosum shape

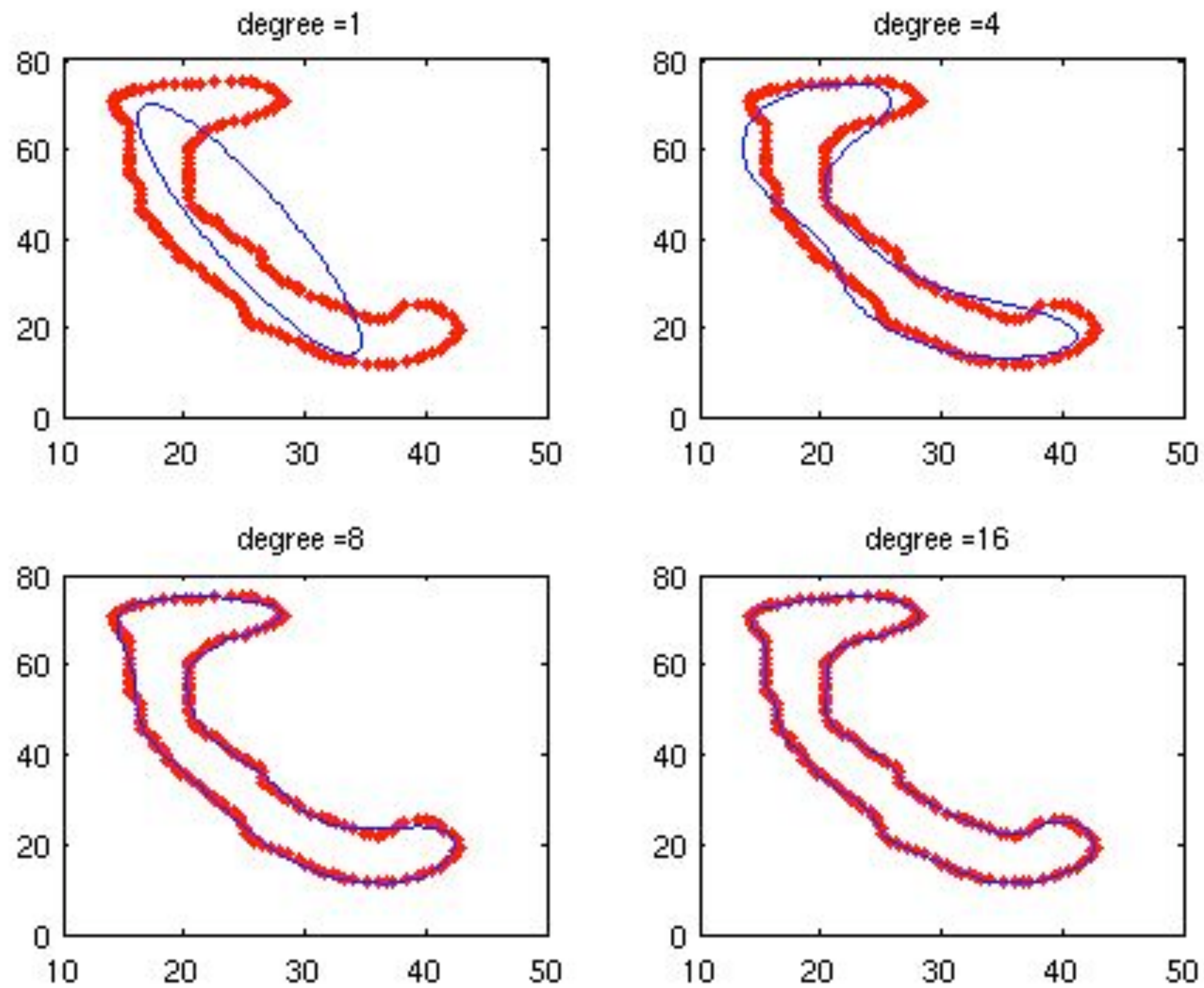

Amygdala modeling

a

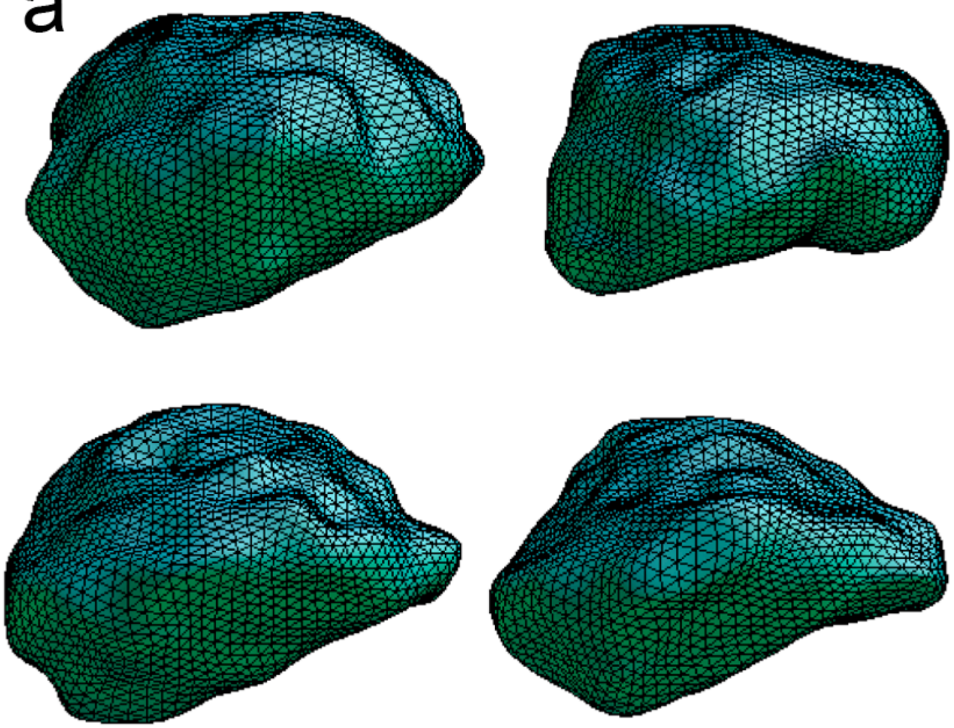

b

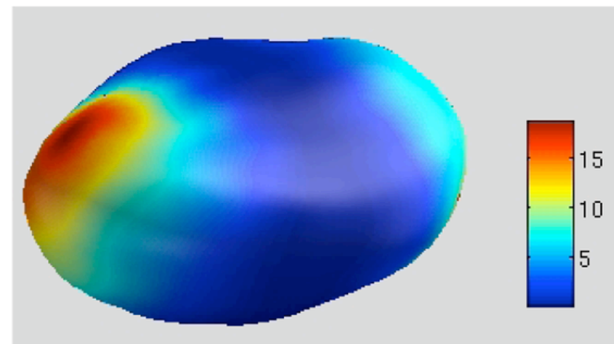

Left Amygdala